

FUNCTIONALIZED NANOPARTICLES AS REMOVABLE  
COATINGS FOR REVERSE OSMOSIS MEMBRANES

---

A Thesis  
Presented to  
the Graduate School of  
Clemson University

---

In Partial Fulfillment  
of the Requirements for the Degree  
Master of Science  
Environmental Engineering and Earth Sciences

---

by  
Megan Anne Smith  
August 2012

---

Accepted by:  
Dr. David Ladner, Committee Chair  
Dr. Cindy Lee  
Dr. Tanju Karanfil

UMI Number: 1518323

All rights reserved

INFORMATION TO ALL USERS

The quality of this reproduction is dependent on the quality of the copy submitted.

In the unlikely event that the author did not send a complete manuscript and there are missing pages, these will be noted. Also, if material had to be removed, a note will indicate the deletion.



UMI 1518323

Copyright 2012 by ProQuest LLC.

All rights reserved. This edition of the work is protected against unauthorized copying under Title 17, United States Code.



ProQuest LLC.  
789 East Eisenhower Parkway  
P.O. Box 1346  
Ann Arbor, MI 48106 - 1346

## ABSTRACT

Reverse osmosis (RO) desalination is increasingly used to produce potable water throughout the world. Despite their promising abilities, membrane filtration processes are limited by fouling. Fouling is a broad term for organics, inorganics, colloids and organisms that interact physically, chemically, or biologically with the membrane surface, resulting in reduced flux and shortened membrane lifespan. There is potential to create a snakeskin-like barrier between the membrane and foulants by electrostatically binding a coating material to the membrane that can be released by pH manipulation, removing foulants in the process. The feasibility of using functionalized nanoparticles as removable adsorptive coatings on RO membranes was evaluated in this study. Several inorganic-polymer composite nanoparticles (NPs) were examined in this study, including titanium dioxide coupled with polydiallyldimethylammonium chloride (polyDADMAC) to impart a positive charge [TiO<sub>2</sub>(+)], titanium dioxide incorporated with polyacrylate to impart a negative charge [TiO<sub>2</sub>(-)] and silver incorporated with polyacrylate, again to incorporate a negative charge [Ag(-)]. PolyDADMAC was used as a positively charged binding layer atop the negatively charged membrane surface to adsorb negatively charged nanoparticles.

A series of concentration experiments was performed for each NP to find the lowest effective concentration for self-assembled coatings. The optimal concentration was then used in a series of kinetic experiments to determine the time required for coatings to assemble. Coating removal experiments were performed over a range of high and low pH values, with attention to indications of chemical alterations to the virgin

membrane. Titrations were run on pairs of membrane samples in an electrokinetic analyzer to measure the surface zeta potential over a range of pH values. While virgin SW30HR had an isoelectric point  $\sim 4$ , the polyDADMAC-coated membrane was completely positive over the pH range tested (3 to 9). When low pH cleaning was used, polyDADMAC was partially removed from the membrane, indicated by an isoelectric point of  $\sim 4.5$ . NP coatings also resulted in changes to the membrane isoelectric point, which was more closely recovered after low pH cleaning. A secondary method for confirming coating and removal was not found, which is an excellent dilemma: coatings are thin enough to be invisible to scanning electron microscopy (SEM) and infrared spectroscopy analysis, but are definitely present as indicated by significant zeta potential changes induced by extremely small quantities of material. It is expected that X-ray photoelectron spectroscopy (XPS) would effectively detect and quantify coatings.

Bench-scale RO experiments were run to test coating efficacy in an applied system. Flux was monitored for deionized water, sodium alginate fouling and acid cleaning. A second deionized water run was performed to determine flux recovery after fouling and cleaning. Membranes were coated similarly to those for electrokinetic studies, but on a larger coupon. RO experiments resulted in 69% recovery of the DI water flux after cleaning a fouled membrane with no coating, compared to a flux of 83% recovery when a NP layer was used.

## DEDICATION

I would like to dedicate this thesis to my Fox and Smith families, both of whom have always been tremendously encouraging and supportive of my educational endeavors. I am honored to be the first in either family to receive a graduate degree in a field I care about so passionately.

To Robyn, my longest and best friend. Despite our differences we have endured so much together, and I look forward to a time when we will not have to Skype and phone to catch up. Some people find soul sisters; I am so lucky to have you as a real one and want to share my daily life with you.

To Toby, the best surprise a family could ask for. You have grown so quickly into such an amazing person. I see so much of myself in you – keep reaching for the stars. They will deliver you to a better life than you can dream. I can't wait to see you through hormones, girlfriends and self-discovery.

To Mom, who passed on the inner chemist. I am so glad you have found work you love and to which you can contribute so much. Keep me posted about that new farm we're starting! I cannot express how much I appreciate your enduring financial and emotional support, though I'm sure you're glad to have your basement back!

To Dad, my student-in-arms. I am so proud of you for stepping up and going back to school when the world decided that 30 years of experience "wasn't good enough". Doubtless that experience has helped tremendously with the process of getting that degree! I can't wait to be at YOUR graduation day soon!

## ACKNOWLEDGMENTS

I would like to acknowledge Dr. David Ladner for reaching out to me and offering this research project, without which I would not have attended Clemson University. I would also like to thank David for the time he dedicated to mentoring, both in group settings and individually.

James Amburgey of the University of North Carolina at Charlotte originally supplied Clarifloc C-308P polyDADMAC polymer and Polydyne, Inc. of Riceboro, GA donated additional material when supplies ran low.

James Eickhoff, Thomas Luxbacher and Vinod Radhakrishnan provided guidance as we learned how to use the SurPASS electrokinetic analyzer and were exceptionally responsive to troubleshooting difficulties throughout the use of the instrument; their help saved us invaluable time and is very much appreciated.

## TABLE OF CONTENTS

	Page
TITLE PAGE .....	i
ABSTRACT .....	ii
DEDICATION .....	iv
ACKNOWLEDGMENTS.....	v
LIST OF TABLES .....	viii
LIST OF FIGURES.....	ix
CHAPTER	
1. BACKGROUND AND INRODUCTION .....	1
1.1 Reverse osmosis membranes.....	3
1.2 Fouling .....	3
1.3 Membrane matrix modifications .....	5
1.4 Permanent surface modification.....	6
1.5 Removable coatings .....	7
1.6 Membrane characterization .....	8
2. RESEARCH OBJECTIVES .....	13
3. MATERIALS AND MATERIAL CHARACTERIZATION .....	14
3.1 Membranes.....	14
3.2 Coating materials.....	16
3.3 Membrane characterization methods .....	18
3.4 Membrane characterization results.....	22
3.5 Polymer and nanoparticle characterization .....	26
4. COATING CONDITION OPTIMIZATION .....	30
4.1 Determining coating concentrations.....	30
4.2 Coating concentration results .....	32
4.3 Membrane coating methods .....	42
4.4 Coating method evaluation.....	43

Table of Contents (Continued)

5.	REMOVAL OF COATINGS.....	48
5.1	Coating removal process.....	48
5.2	Coating removal results.....	49
6.	BENCH SCALE RO FOULING EXPERIMENTS.....	58
6.1	Experimental design.....	58
6.2	RO methods and additional materials.....	59
6.3	Bench scale RO results.....	62
7.	CONCLUSIONS AND RECOMMENDATIONS.....	70
7.1	Conclusions relating to research objectives.....	70
7.2	Future work recommendations.....	74
	APPENDICES.....	79
A:	Additional Images.....	80
B:	SurPASS Adjustable Gap Cell: Standard Operating Procedures.....	84
C:	Bench Scale RO for Membrane Coatings: Standard Operating Procedures.....	87
	REFERENCES.....	90

## LIST OF TABLES

Table		Page
3.1	Calibration concentrations for ICP-OES analysis.....	22
3.2	ICP data for Ag standards and triplicate working solutions diluted to 0.5%.....	28
3.3	ICP data for Ti standards and triplicate working solutions diluted to 50%.....	29
5.1	Comparison of single measurement electrokinetic data for coating materials. Change in zeta potential for acid and base cleaning is reported as the difference between the coated membrane and after cleaning..	51
6.1	Experimental matrix for bench scale RO experiments using SWC5 membranes .....	59
6.2	Average flux normalized to SWC5 DO water experiment after each stage of RO filtration .....	68

## LIST OF FIGURES

Figure		Page
3.1	Structures of m-phenylenediamine (a) and trimesoyl chloride (b), the precursors to PA TFC surface layers.....	15
3.2	Structure of cross-linked polyamide .....	15
3.3	Monomer structure of diallyldimethyl ammonium chloride .....	16
3.4	Sketch representation of NP surface charges imparted by polyacrylate (a) and polyDADMAC (b) .....	18
3.5	General representation of adjustable gap cell setup .....	19
3.6	Zeta potential curves for SW30HR, SWC4 and SWC5 TFC PA membranes. Breaks in the titration curve resulted from the separation of acid and base titrations, which provided separate sets of data .....	23
3.7	Titration curves of three SW30HR samples. Titration curves have very similar shapes but vary slightly in zeta potential, as seen in the June and February data. The January titration was performed after the membrane had been stored at 4°C for over 3 months. ....	24
3.8	SW30HR samples in HCl solutions of varying strength for 30 min. Strong acid significantly altered the zeta potential while weaker acid solutions did not .....	25
3.9	Zeta potential drop of pH 1 acid washed SW30HR compared to virgin SW30HR and SWC5 membranes.....	26
4.1	PolyDADMAC coating on SWC4 membrane. The polymer coating significantly altered the surface chemistry, creating a positively charged membrane surface .....	33
4.2	PolyDADMAC coatings of 2%, 1% and 0.2% on dry SW30HR membranes. All coatings impart a strong charge; there is no notable difference between 0.2% and 1%, and little difference at 2%. ....	34

List of Figures (Continued)

Figure	Page
4.3 Effects of 2.1 mg/L, 4.2 mg/L, 10.6 mg/L and 21.2 mg/L TiO <sub>2</sub> (+) on membrane surface charge compared to the uncoated SW30HR membrane .....	35
4.4 TiO <sub>2</sub> (+) NP coatings for two sets of experiments. Significant differences could be attributed to changes in NP stock solution or heterogeneity of the membrane surface.....	36
4.5 Charge density of polyDADMAC coating compared to TiO <sub>2</sub> (+) NP coating, which was functionalized with polyDADMAC .....	37
4.6 Reduction in surface charge by Ag(-) NPs adsorbed to polyDADMAC. As expected, the higher the NP concentration, the lower the zeta potential. Error bars represent a standard deviation from 12 measurements .....	38
4.7 20 mg/L Ag(-) coatings compared to virgin SW30HR.....	40
4.8 SEM image of Ag(-) aggregation on SW30HR membrane. Aggregates are very large, up to 6 μm in size. NPs are ~10 nm.....	41
4.9 TiO <sub>2</sub> (-) coatings on polyDADMAC membranes from two experiments. Significant deviation in shape and zeta potential were observed.....	42
4.10 Titrations for polyDADMAC-coated SW30HR show that a dry membrane coated statically at low temperature had a more positive charge than a wet membrane coated dynamically at room temperature .....	44
4.11 Control coatings on SW30HR. TiO <sub>2</sub> (+) did not adsorb to polyDADMAC; TiO <sub>2</sub> (-) and Ag(-) appear to have adsorbed to SW30HR despite carboxyl groups promoting electrostatic repulsion.....	45

List of Figures (Continued)

Figure	Page
4.12 SEM images of virgin SW30HR (left) and polyDADMAC-coated SW30HR (right). PolyDADMAC coating appeared to fill in the loop and valley structure of the membrane.....	46
4.13 ATR-FTIR of polyDADMAC and negatively charged NP coatings did not indicate any change in surface chemistry .....	47
5.1 Acid cleaning of polyDADMAC-coated SW30HR resulted in significant but incomplete removal of the polymer.....	50
5.2 Acid cleaning of TiO <sub>2</sub> (+) coatings. Acid cleaning resulted in complete removal of NPs for all acid concentrations investigated.....	52
5.3 SEM images of uncoated SW30HR (a), Ag(-)-coated SW30HR (b), pH 1 acid-cleaned Ag(-)-coated SW30HR (c) and pH 13 base-cleaned Ag(-)-coated SW30HR (d).....	54
5.4 Electrokinetic behavior of Ag(-) coatings after acid cleaning .....	55
5.5 Electrokinetic behavior of TiO <sub>2</sub> (-) coatings after acid cleaning .....	57
6.1 Diagram of reverse osmosis bench scale filtration system .....	60
6.2 Comparison of DI water flux. Uncoated SWC5 had the highest flux with polyDADMAC-coated and Ag(-)-coated fluxes slightly lower.....	64
6.3 Fouling of virgin, polyDADMAC-coated and Ag(-)-coated membranes. Somewhat less fouling occurred on the coated membranes, resulting in 10% higher flux .....	65

## List of Figures (Continued)

Figure		Page
6.4	Flux recovery after acid cleaning. PolyDADMAC coating gives slight improvement in flux recovery, but Ag(-) coating notably increases post-cleaning flux .....	66
6.5	Comparison of DI water flux for Ag(-) coated SWC5 membranes. The third data set dropped suddenly by approximately 5% flux after 1.5 hr, which cannot be explained with the data available .....	67
6.6	Comparison of SWC5 fouling experiments. Fouling experiments were more varied than DI water flux. Different rates of fouling and flux decline are observed .....	67
6.7	Full RO experiments. PolyDADMAC and Ag(-) coatings had lower initial flux and slower fouling. Ag(-) had notable flux improvement after cleaning .....	69
7.1	Expected desorption mechanisms for positive materials at low pH (a) and negative particles at high pH (b). polyDADMAC and TiO <sub>2</sub> (+) were expected to detach from the membrane via mechanism (a) while negatively charged NPs were expected to detach from the polyDADMAC layer via mechanism (b) .....	74

## **CHAPTER ONE**

### **BACKGROUND AND INTRODUCTION**

Drinking water quality is a major health concern throughout the world. Dwindling supplies of potable water mandate the reuse of water and purification of groundwater and surface water prior to use (Shannon et al., 2008). As human populations continue to expand and concentrate in coastal areas, many communities around the globe only have access to briny, salty or polluted water. Membrane filtration systems can remove a significant amount of undesirable biological and chemical species, including salt; typically have a smaller footprint than distillation systems; and are more effective at contaminant removal than standard filtration. These attributes make membrane filtration systems a conceptually appealing solution.

Four levels of membrane filtration are available for water purification purposes: microfiltration (MF) removes microbes and particles typically larger than 0.1  $\mu\text{m}$ ; ultrafiltration (UF) removes macromolecules such as proteins, polysaccharides, larger molecular weight pesticides and pharmaceuticals; nanofiltration (NF) removes smaller organic pollutants such as chlorinated pesticides and multivalent ions like calcium, magnesium, and iron; and reverse osmosis (RO) removes monovalent ions such as sodium and chloride. NF and RO are both pressure-driven processes, requiring robust membrane materials to withstand high operating pressures. Thin-film composite membranes are frequently used, with a thin active layer supported by a thick, strong and inert backing layer. This endurance requirement has until recently led to membrane

development focused on building stronger and longer-lasting membranes. Within the past several decades, the focus on membrane lifetime has led to research in fouling resistance, but membrane cleaning remains an issue (van der Bruggen et al., 2008).

RO technology is widely used for desalination of seawater and brackish water, both of which may contain large quantities of organic matter and marine organisms that may contribute to chemical and biological fouling of the membrane. For example, the sheer mass of bacteria present in red tides can cause significant fouling in desalination plants and frequently require the plant to cease operation until the bloom has dispersed (Petry et al., 2007). In a study using NF for seawater desalination, 20% fouling was observed over a three-day period, making the operation unsustainable (Harrison et al., 2007). Fouling is a hindrance to the RO process, frequently requiring the system to be offline for cleaning. Commercial membranes have been developed to reduce the rate of fouling or prevent certain types of fouling, but no indefinitely fouling-resistant membrane has been achieved.

Negatively charged NPs have been coupled with RO membranes to investigate the feasibility of using electrostatic interactions to attach and release self-assembled coatings of these materials. Electrostatic interactions between membranes and coating materials were manipulated to cause adsorption and desorption by varying the pH. On negatively charged membranes such as polyamide, an increase in proton concentration (decreasing pH) protonates the carboxyl groups on the membrane, neutralizing the membrane once a critical proton concentration is reached. Surface charge continues to increase beyond the isoelectric point as protons collect around electron density at surface

carboxyl groups. The polymer polydiallyldimethylammonium chloride (polyDADMAC) was selected for its strong positive charge to serve as a binding layer between the negatively charged membrane and negatively charged NPs. This project developed coating, removal and characterization methods and examined the advantages and drawbacks of each.

### **1.1 Reverse osmosis membranes**

Reverse osmosis is the most globally employed desalination technology, with half of 15,000+ desalination plants employing RO processes (Greenlee et al., 2009). Successful development of membrane materials, followed by further modifications to increase membrane performance, played a crucial role in the global application of this technology. Many commercial RO membranes are thin film composite (TFC) polyamide (PA) membranes, which consist of three layers: a polyester supportive backing layer (120-150  $\mu\text{m}$  thickness), a microporous polysulfone interlayer (40  $\mu\text{m}$ ) and an extremely thin polyamide active layer on the membrane surface (0.2  $\mu\text{m}$ ) (Petersen & Cadotte, 1990). Commercial materials are developed for effectiveness despite heterogeneity caused by the manufacturing process, and active layers can vary chemically across the membrane as well as throughout the depth of the surface layer (Coronell et al., 2011).

### **1.2 Fouling**

While RO is low-cost compared to other desalination techniques, the process is hindered by fouling (Goosen et al., 2004). Seventy percent of seawater RO plants in the Middle East have biofouling issues and 83% of plants surveyed in the United States reported fouling problems as well (Yang et al., 2009). A wide range of materials can foul

membranes, including organics (e.g. natural organic matter [NOM] and humic acid), inorganics (e.g. scale-forming salts like barium sulphate; van de Lisdonk et al., 2000), biopolymers (e.g. proteins and polysaccharides making up extracellular polymeric substances [EPS]), and biological organisms themselves (e.g. *Mycobacterium* sp.; Campbell et al., 1999). Foulants can originate as soluble materials in the feed water that deposit on the membrane, or they can be colloidal or particulate in nature before depositing. Inorganic solutes can precipitate on the surface of the membrane, or precipitate to form particles first, then deposit. Organic foulants tend to be the most common due to their prevalence in feed waters of all types and their complex interaction chemistries. Organics can adsorb to the membrane surface as well as within the pores of MF, UF and NF membranes (Lee et al., 2005; Braghetta et al., 1998; Cho et al., 1998; Hong et al., 1997). The surface chemistry of the membrane and the chemistry of the feed solution both factor into fouling effects, as well. Negatively charged membrane materials tend to incur less biological fouling due to electrostatic repulsion effects, but cation bridging, surfactant boundary formation and pH changes can all increase fouling (Childress and Elimelech, 1996).

The wide variety of materials that cause membrane fouling, which can result in several types of fouling within a single system, makes it difficult to design a membrane material impervious to all types of fouling. Our research, therefore, aims not to develop a membrane material, but a coating that acts as a snakeskin-like barrier such that all types of fouling are removed when the coating is washed away. The coating could then be reapplied to refresh the barrier layer.

### 1.3 Membrane matrix modifications

One strategy for reducing fouling while maintaining membrane flux is modification of the membrane matrix before or after casting. NPs have become a promising set of materials due to their small size, affinity for polymer binding and attractive properties such as biocidal silver and photoactivated titanium dioxide (Kim and van der Bruggen, 2010; Soroko and Livingston, 2009; Yan et al., 2006).

Polymer-functionalized metal composite NPs are a type of nanomaterial with properties that could be of interest. These NPs are typically given charge by a carboxyl- or amino-functionalized polymer; however, research to this point has focused on pure material NPs and only one publication could be found regarding functionalized NP use in membrane filtration (Jadav et al., 2010). Pure NP materials most often described in the literature are titanium dioxide ( $\text{TiO}_2$ ), alumina ( $\text{Al}_2\text{O}_3$ ), silver (Ag), silica and zirconia. There have been a number of self-assembly poly(ether)sulfone and polysulfone UF membranes that use  $\text{TiO}_2$  NPs as modifiers; an optimized amount of NPs is added to the casting solution before preparing the membrane itself (Luo et al., 2005). Jeong et al. (2007) have created mixed matrix RO membranes incorporating various concentrations of 50-150 nm zeolite NPs in the casting solution. These mixed matrix membranes had improved permeability over PA membranes also formed in the laboratory, indicating that inclusion of nanomaterials in the membrane active layer may be a promising avenue.

The membrane surface can also be modified by dipping the membrane in a concentrated NP solution. These studies have been done with carefully controlled preparations of  $\text{TiO}_2$  NPs that were pre-analyzed for particle size (Bae et al., 2006). Both

matrix incorporation and dip coating methods seem promising for application to many membrane types as well as different types of NPs. Some concerns have been noted such as the aggregation of NPs when the concentration is too high, resulting in a reduction of permeability and flux (Soroko and Livingston, 2009; Luo et al., 2005; Yang et al., 2007). Another concern noted by Taurozzi et al. (2008) regarded significant silver NP loss from the matrix during initial wetting of the membrane. There have also been encouraging results from these investigations. It has been reported that addition of nano-sized alumina did not affect the structure of the membrane or its pores (Yan et al., 2006). The mechanical properties of the membrane actually improved and later studies explored the optimal concentrations for enhancing membrane strength and fouling resistance.

#### **1.4 Permanent surface modification**

Anti-fouling research for NF and RO membranes is currently progressing toward permanent modification by covalent bonding of coatings to the membrane surface. Polymer surface modification typically makes the surface more hydrophilic, since lower fouling potential is generally correlated to greater hydrophilicity (Ba et al., 2010; Louie et al., 2006). Over the past decade researchers such as Kilduff and Belfort have made significant developments in surface modification, developing a graft polymerization technique that employs UV light or plasma to create reactive sites on the membrane surface that are then exposed to a coating material, creating permanent chemical bonds between a membrane and the polymer coating (Zhou et al., 2009; Kilduff et al., 2003; Minghao et al., 2012). These modifications tend to be highly specialized, targeting certain

chemical or biological species types instead of serving as a one-stop filtration unit, and reduction of membrane fouling has been questioned (van der Bruggen et al., 2008).

### **1.5 Removable coatings**

Permanent surface modification is a useful means of changing fouling behavior, but even the most resistant membranes can eventually be fouled. This is especially true for feed waters like wastewater and surface water, which contain a wide variety of organic and inorganic material. An ideal removable membrane coating would reverse fouling no matter the foulant characteristics. This would reduce the impact of membrane cleaning, leading to longer lasting membranes and lower overall system cost. The use of NPs in membrane systems has been reported in the literature and shows great promise with improved membrane mechanics and permeability as well as strong evidence of fouling resistance. The primary focus of this research will be to develop a system of NPs and membranes where the NPs can be deposited and subsequently removed to yield a regenerable system.

Polyvinyl alcohol has been investigated as a removable coating paired with a positively charged NF membrane to create a coating that can be removed with a simple acid cleaning (Ba et al., 2010). This combination was a highly effective coating, with flux recovery of nearly 100% after low pH cleaning. The interaction of functionalized nanoparticles with polymeric membranes has also been investigated, with the intention of removing the NPs using membrane processes (Ladner et al., 2012). NPs were effectively removed and demonstrated interesting adsorption characteristics, which led to the development of the work performed for this thesis.

## **1.6 Membrane characterization**

Some background on membrane characterization methods is included here to understand how the techniques used in this study fit into the literature of the field. Physicochemical properties of membranes and effects of fouling, coatings and modifications are characterized using an array of techniques from materials science, chemical engineering and traditional chemical analysis. Chemical (zeta potential, elemental composition and functional groups present) and physical (hydrophilicity, flux and roughness) properties are observed and compared to virgin membrane to determine beneficial or disadvantageous effects. Many techniques are available for RO membrane characterization and their use depends on the properties being investigated. For chemical analysis, zeta potential indicates the overall surface charge and isoelectric point, attenuated total reflectance Fourier-transform infrared (ATR-FTIR) spectroscopy determines functional groups associated with the membrane surface and foulants, and energy-dispersive X-ray spectroscopy (EDS) determines elemental composition. For physical analysis, contact angle measurement indicates hydrophilicity of the membrane material, bench-scale filtration determines baseline flux and flux effects of modification, atomic force microscopy (AFM) visualizes surface roughness, and scanning electron microscopy (SEM) visualizes the membrane surface and any coating or foulant aggregation.

### *1.6.1 Zeta potential*

Electrokinetic characteristics of reverse osmosis membranes have a significant influence on fouling performance and contaminant retention. Polyamide membranes,

which have a slightly negative surface charge at neutral pH, can electrostatically repel negatively charged functional groups common to natural organic matter. In the presence of positively charged functional groups, however, the membrane charge is a hindrance and encourages electrostatic binding that can be difficult to remove (Ba et al., 2010). Fundamental studies over the past several decades have investigated the chemical properties of the membrane surface layer (Childress and Elimelech, 1996; Childress and Elimelech, 2000). Significant progress has been made toward understanding the complex chemistries involved in membrane surface interactions, but fouling continues to plague desalination plants and other membrane filtration processes. The mechanisms of fouling and means of preventing it are still being explored. Zeta potential characterization of membrane cleaning studies has also been undertaken, though these studies use complex cleaning agents as used in large-scale operations and recommended by manufacturers (Al-Amoudi et al., 2007).

The work conducted for this thesis included a SurPASS electrokinetic analyzer manufactured by Anton Paar GMBH. The electrokinetic properties of the membrane surface are determined by forcing an electrolyte solution through a sample cell containing the material of interest; electrodes at each end of the sample cell measure the resulting streaming current and zeta potential is calculated (Buksek et al., 2010). The Fairbrother-Mastin (F-M) approach to calculating zeta potential ( $\zeta$ ), given in Equation 1, improves upon the earlier Helmholtz-Smoluchowski (H-S) approach, accounting for phenomena in the instrument that affect the reported measurements (Buksek et al., 2010).

$$\zeta = \frac{dI}{dp} \times \frac{\eta}{\varepsilon \times \varepsilon_0} \times \frac{L}{A} \quad (1)$$

Here  $dI/dp$  is the measured slope of streaming current versus pressure,  $\eta$  is the electrolyte viscosity,  $\varepsilon$  is the dielectric constant of the electrolyte,  $\varepsilon_0$  is the vacuum permittivity,  $L$  is the length of the streaming channel, and  $A$  is the cross-sectional area of the streaming channel.

### 1.6.2 Scanning electron microscopy and energy-dispersive X-ray spectroscopy

Scanning electron microscopy (SEM) is used to visualize the membrane surface and determine whether coatings or fouling have caused considerable changes to the surface structure (Cahill et al., 2008). Polymeric materials are not electrically conductive and do not contribute to the backscattering and secondary electrons that scanning electron microscopy relies upon to produce an image, so membranes must be sputter-coated with gold, platinum or another heavy element (Michler, 2008).

Energy-dispersive X-ray spectroscopy (EDS) is an analytical technique commonly coupled with scanning or tunneling electron microscopes to determine the elemental composition of solid samples. In membrane systems, EDS can be used to confirm the presence of inorganic contaminants or uncharacteristic C:N:O ratios. For this research, EDS is intended to detect the metallic components of the nanoparticles, indicating the presence of the nanoparticle layer. The requirement for sputter coating and the small quantities of coating material on the membrane surface complicate the results of EDS analysis.

### *1.6.3 Attenuated total reflectance Fourier-transform infrared spectroscopy*

ATR-FTIR spectroscopy is used to confirm functional groups present in the membrane, such as the carboxyl and amine groups expected for a polyamide membrane, or to determine functional groups associated with natural organic matter (NOM) or other foulant materials (Cho et al., 1998). In RO research, ATR-FTIR is often used to confirm that the membrane surface, coating or foulant is performing as expected (Coronell et al., 2010; Tang et al., 2009a; Tang et al., 2007). This technique is not often the primary analysis of membranes or membrane coatings, though some studies such as Belfer et al. (1998) have demonstrated the benefits of utilizing peak emergence and absorbance changes for assessing membrane coatings. Proper accessories and setup of the instrument, such as crystal selection, angle of incidence and atmosphere purging, are critical for ATR-FTIR use as the primary instrumentation for analysis. Without extremely sensitive instrumentation, it is very difficult to discern the small quantities of coating layers over the dominant vibrational bands of the polysulfone support membrane and ATR-FTIR is of limited benefit (Gabelich et al., 2005).

### *1.6.4 Contact angle measurements*

Contact angle measurement is used to assess the hydrophilic character of a membrane material and the change resulting from membrane modification or coating. The sessile drop method is most commonly used for membrane analysis. This method involves placement of a liquid droplet onto the membrane surface and photographic visualization with a contact angle goniometer (Hurwitz et al., 2010). Software is used to determine the contact angle of the drop on the membrane. Titrations can be performed by

varying the pH of droplets, allowing characterization of membrane surface chemistry throughout a range of pH values. The type of liquid used in the droplet can also be varied, and a “wettability” parameter can be identified based on the affinity of the membrane for particular liquids (Brant and Childress, 2004). A second technique that can be applied to membrane surface characterization is the captive bubble method, in which the surface is immersed face-down in a liquid and a gas bubble is released onto the membrane surface from below (Drelich et al., 1996).

In both cases, the shape of the drop/bubble is metastable and can be affected by outside pressures, evaporation and other factors. There is a phenomenon called hysteresis well described by Gao and McCarthy (2006). In basic terms, an increasing droplet will cover a defined area with changing contact angle until reaching a certain volume, at which point it will increase in area with a constant contact angle; a decreasing droplet will decrease in volume with a changing contact angle until reaching a critical volume, at which point the area will decrease with a constant contact angle. To account for both aspects of this phenomenon, contact angle measurements often include additions and subtractions of drops/bubbles to find the constant contact angle (Drelich et al., 1996). Apolar compounds can also be used to serve as an indicator of hydrophobicity; for RO membranes, large contact angles indicating a decrease in hydrocarbon affinity would be desired (Brant and Childress, 2002; Subramani and Hoek, 2008).

## CHAPTER TWO

### RESEARCH OBJECTIVES

This project was designed to evaluate the interactions between reverse osmosis membranes and nanoparticle coatings and to determine whether the coatings could be removed from the membrane. The specific objectives were:

1. ***Determine appropriate conditions for self-assembly of polymer and nanoparticle coatings on reverse osmosis membranes.*** Experimental conditions such as working concentrations of polymer and nanoparticles, time required for coating and methods for applying coatings needed to be identified.
2. ***Determine appropriate conditions for coating removal.*** Two possible desorption scenarios were anticipated: desorption of the nanoparticles from the polyDADMAC coating, and desorption of the polyDADMAC coating from the membrane. Experiments investigated whether high or low pH cleaning was more effective for coating removal.
3. ***Use zeta potential titrations to detect the presence of self-assembled coatings.*** The Anton-Paar SurPASS electrokinetic analyzer was purchased for this project. Optimization of instrument methods was a critical component of this project.

## CHAPTER THREE

### MATERIALS AND MATERIAL CHARACTERIZATION

Significant developments have been made regarding permanent membrane modifications and improved removal of target compounds, but removable coating design has not been widely reported in the literature to date. Because removable coating design has not been widely studied, it was necessary to determine how best to coat the membranes, remove coatings and to perform concentration studies to optimize the later experiments. Ultrapure water (DDI) from a Super-Q Plus System (Millipore, Bedford, MA) was used for all solutions, sample preparation and electrokinetic analysis. The use of the words “adsorption” in this document refers to electrostatic adsorption unless otherwise noted.

#### 3.1 Membranes

Reverse osmosis membranes from two manufacturers were used: SW30HR from Dow Filmtec, a subsidiary of the Dow Chemical Company (Midland, Michigan) and SWC4 and SWC5 from Hydranautics, a Nitto-Denko company (Oceanside, California). All membranes are thin film composite (TFC) polyamide (PA) formed by cross-linking of *m*-phenylenediamine and trimesoyl chloride, shown in Figures 3.1 and 3.2. SW30HR is commercially coated with a polyvinyl alcohol surface layer while SWC4 and SWC5 are uncoated (Tang et al., 2009b).

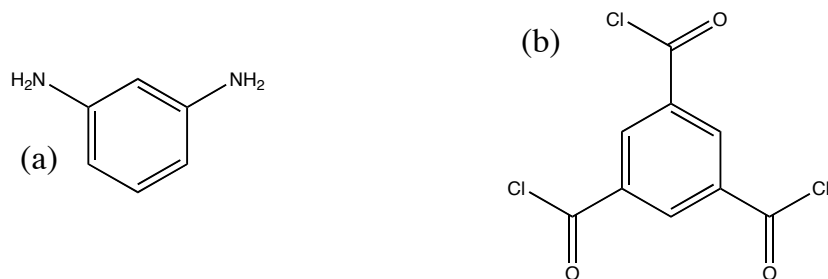


**Figure 3.1.** Structures of m-phenylenediamine (a) and trimesoyl chloride (b), the precursors to PA TFC surface layers.

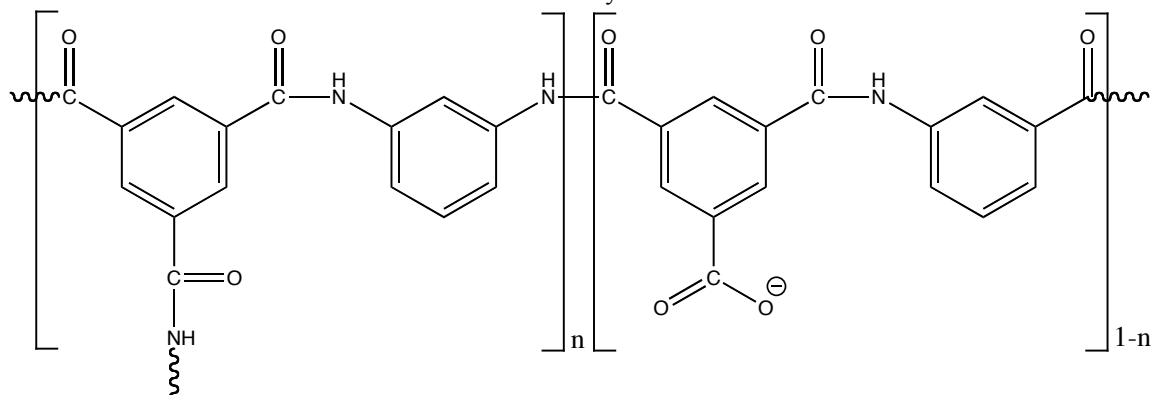


**Figure 3.2.** Structure of cross-linked polyamide.

SW30HR and SWC4 were obtained as flat sheets prior to 2009 and stored dry in cardboard tubes to protect from light. Membrane material was cut from the flat sheet, wetted with DDI water and stored at  $4^\circ\text{C}$  in DDI water that was changed at least biweekly. SWC5 was purchased as a complete, tested RO module in late 2011 and stored at  $4^\circ\text{C}$  in DDI water once opened. Coupons for experiments were cut and placed in DDI water, then stored at  $4^\circ\text{C}$  at least overnight and up to several weeks with DDI water changed weekly.

## 3.2 Coating materials

### 3.2.1 PolyDADMAC positively charged polymer

PolyDADMAC was selected for its low cost and widespread availability as well as its strong positive charge. It is widely used as a flocculent in water treatment and, if effective, would be easy to implement. The monomer structure is shown in Figure 3.3. PolyDADMAC has been demonstrated to interact with polyamide membranes in favorable ways regarding these research goals, including deposition on the membrane in thin layers and minimal flux reduction after deposition (Gabelich et al., 2005). One drawback to polyDADMAC in a water treatment context is that it has recently been implicated as a disinfection byproduct precursor; it leads to n-nitrosodimethylamine (NDMA) formation, in particular (Park et al., 2009). The polyDADMAC used in this study was 20% (w/v) Clarifloc C-308P, donated by James Amburgey of UNC-Charlotte and by Polydyne, Inc. (Riceboro, GA). C-308P has an average molecular weight range of 80-120 kDa. The 20% stock solution was used as received. A graduated cylinder was used to measure polyDADMAC and was rinsed several times into the final solution to ensure complete transfer of the slightly viscous polymer.

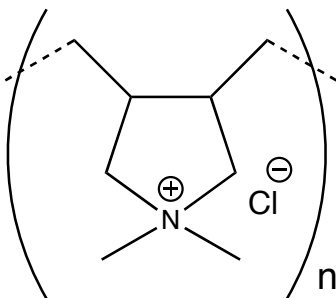


**Figure 3.3.** Monomer structure of diallyldimethyl ammonium chloride.

### 3.2.2 *Functionalized silver and titanium dioxide nanoparticles*

Functionalized nanoparticles were purchased from Vive Nano, Inc. (Ontario, Canada). General representation of the NP surface is shown in Figure 3.4 for negative (a) and positive (b) charges. Negatively charged silver [Ag(-)] was functionalized by the manufacturer with a sodium polyacrylate derivative and received in aqueous solution of 1 g/L Ag. A 0.1 g/L working solution of Ag(-) was prepared by a tenfold dilution of the stock solution, which was used as received.

Negatively charged titanium dioxide [TiO<sub>2</sub>(-)] was functionalized by the manufacturer with a polyacrylic acid derivative and a polystyrene sulfonate derivative and arrived as 18.3% w/w powder (lot PB75). Stock solution was prepared by dissolving 0.100 g powdered TiO<sub>2</sub>(-) into 100 mL DDI water for a final concentration of 0.184 g Ti/L.

Positively charged titanium dioxide [TiO<sub>2</sub>(+)] was functionalized by the manufacturer with polyDADMAC and arrived as at 20% w/w powder (lot PB75). Stock solution was prepared by dissolving 0.106 g powdered TiO<sub>2</sub>(+) into 100 mL DDI water for a final concentration of 0.212 g Ti/L.

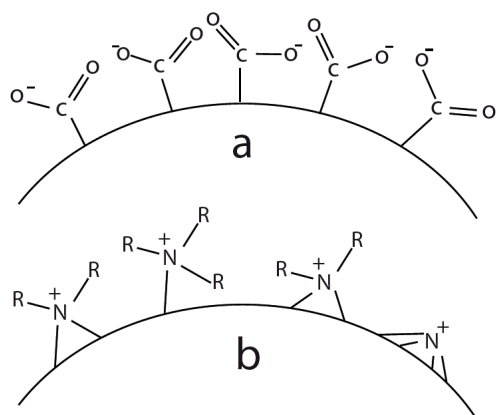


**Figure 3.4.** Sketch representation of NP surface charges imparted by (a) polyacrylate and (b) polyDADMAC.

### 3.3 Membrane characterization methods

#### 3.3.1 Zeta potential

##### 3.3.1.1 Instrumentation

Surface zeta potential was measured with a SurPASS electrokinetic analyzer (Anton-Paar, Graaz, Austria). VisioLab software version 2.10 was provided for instrument control and upgraded to version 2.20 before experiments started. The instrument was purchased with a clamping cell sample holder. This measuring cell required membrane coupons of 55 mm x 25 mm and used only 9% of the total membrane area, while the contribution of the remaining membrane area to membrane body conductance was unaccounted for (Bukšek et al., 2010). The adjustable gap cell (AGC) sample holder, which required smaller membrane coupons of 10 mm x 20 mm and used 100% of the membrane surface area for measurement, was purchased in spring 2011 due to improvements in measurement reliability and was used from May 2011 onward (Figure 3.5).

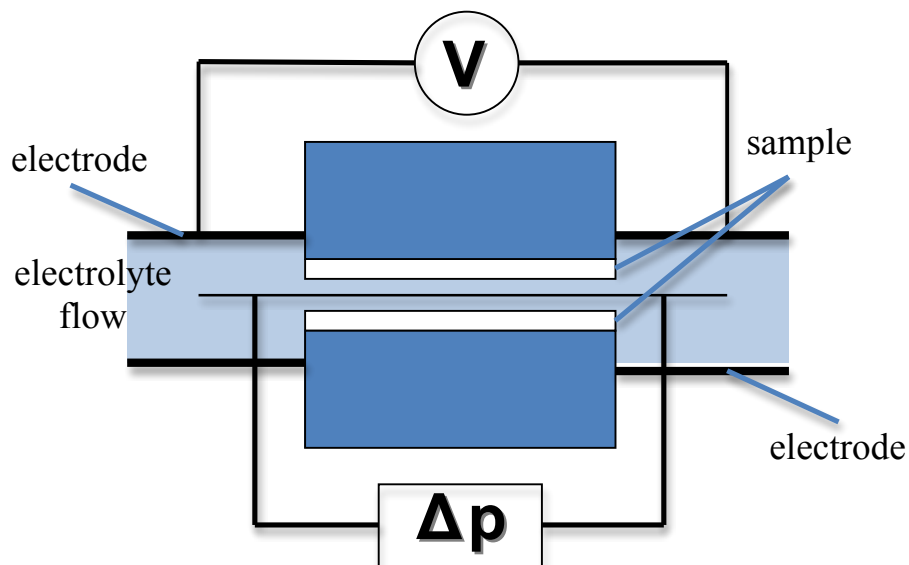


**Figure 3.5.** General representation of adjustable gap cell setup.

### 3.3.1.2 Chemicals for analysis

Potassium chloride salt was purchased from BDH Chemicals, Ltd, a subsidiary of VWR International (Radnor, PA), and used as received. A stock KCl solution of 0.1 M was prepared with DDI water and kept in the dark at room temperature. The stock solution was vacuum filtered with a 0.22  $\mu\text{m}$  polyvinylidene fluoride filtration membrane (Millipore, Billerica, MA). Working solutions of 0.001 M KCl were prepared before each titration by diluting 10 mL of stock solution into 1 L of ultrapure water and vacuum filtering through a 1  $\mu\text{m}$  Nylasorb nylon membrane (Pall Life Sciences, Ann Arbor, MI) to eliminate dust and other particulates.

Acid titrations used 0.1 M hydrochloric acid (HCl), prepared by diluting 8 mL of 37% laboratory grade HCl (BDH Ltd, Radnor, PA) into 1 L DDI water. Base titrations

used 0.1 M sodium hydroxide (NaOH), prepared by dissolving 4 g NaOH pellets (EMD Millipore, Billerica, MA) in 1 L DDI water.

#### *3.3.1.3 Titrations*

The AGC was assembled as instructed in the instrument user manual. DDI water was used for filling and rinsing of the instrument, gap adjustment and flow check. KCl electrolyte solution was flushed through the instrument before each measurement. The Adjustable Gap Cell template file in VisioLab software was used for all AGC measurements in “pH titration” mode, modified for a maximum pH of 9 for base titrations.

During initial experiments on the AGC, titrations were run from acidic (pH ~3) to basic (pH ~10-11) or vice versa. After being advised against single titrations because of the ionic strength of the feed solution, titrations were split into two “halves”, an acid titration from ambient DDI pH (~5.5) to 3 and a base titration from ambient pH to 9. Acid titrations were executed first for all samples. When the acid titration finished, the instrument was rinsed with three changes of DDI water to eliminate electrolyte in the system. KCl solution was flushed through before the base titration was started. Upon completion of the base titration, the instrument was rinsed with DDI water until the baseline pH (~5.5) was restored. The *Empty* command was used to clear the tubing and conclude the experiment. Used membranes were discarded.

#### *3.3.1.4 Single measurements*

Single measurements were performed to assess instrument variability and occasionally to perform rapid analysis of surface potential at a predetermined pH.

Samples were prepared as for titration measurements. In VisioLab software the “single measurement” mode was selected and 12 measurements were taken to decrease instrument noise.

#### *3.3.1.5 Instrument maintenance*

Routine instrument maintenance was performed for the SurPASS over the course of the project. The conductivity meter was calibrated every three months or before use if the instrument had been unused for at least a week. The pH meter was stored in 3 M KCl when not in use and was calibrated monthly. Titration unit tubing was rinsed monthly to eliminate air bubbles in the lines. The sample cell was fully disassembled and cleaned with dilute isopropyl alcohol after all SW30HR experiments concluded.

#### *3.3.2 Attenuated total reflectance Fourier-transform infrared spectroscopy*

ATR-FTIR spectroscopy was used to determine whether the coatings could be detected, as would be expected if quantities sufficient to foul the membrane were present. A Nicolet 6700 FTIR (Thermo Scientific, Waltham, MA) fitted with a diamond Smart-iTR plate was used with a scanning resolution of 2, giving a total of 32 scans per spectrum.

#### *3.3.3 Scanning electron microscopy*

SEM was employed to visualize the effects of the coating and removal processes. Membrane samples were sputter-coated with gold using a Hummer 6.2 sputtering machine (Anatech Ltd., Battle Creek, MI) prior to analysis. Images were taken at magnification of 2.5 k and 10.0 k with a tabletop TM3000 unit (Hitachi High Technologies America, Inc., Dallas, TX). High-resolution images were taken at

magnification 10 k and 100 k with a variable pressure Field Emission SEM SU6600 microscope (Hitachi High Technologies America, Inc., Dallas, TX).

### 3.3.4 Inductively coupled plasma optical emission spectroscopy (ICP-OES)

Nanoparticle solution concentrations were quantified using ICP-OES. Three samples of each NP working solution were dissolved in 5% HNO<sub>3</sub> for 24 hours before analysis. A 1000 ppm (1000 mg/L) titanium standard was used for Ti NPs and a multi-element standard containing 10 ppm (10 mg/L) silver was used for Ag NPs. Titanium NPs were diluted 1:1 into HNO<sub>3</sub> for an expected concentration of 0.1 g Ag/L; the 0.1 g/L working solution of Ag NPs was diluted to 0.5% for an expected final concentration of 0.5 mg Ag/L. Calibration concentrations are shown in Table 3.1.

**Table 3.1.** Calibration concentrations for ICP-OES analysis.

[Ti] (ppm)	[Ag] (ppm)
0	0
10	0.01
25	0.025
100	0.05
250	0.1

## 3.4 Membrane characterization results

Each membrane had a unique zeta potential curve and isoelectric point. Breaks in the titration curve were caused by the separation of acid and base titrations, which resulted in two sets of data for the pH range 3-9. Each data point is the averaged value from four measurements; the average standard deviation for titration curves was  $\pm 2$  mV and consistent throughout the experiments. Figure 3.6 shows the characteristics of each membrane involved in this study. SWC5 and SWC4 show similarities in zeta potential at

operational pH for desalination (approximately pH 8), but the charge of SWC5 is much lower than SWC4 at acidic pH. The isoelectric point of SWC5 is roughly 3, while SWC4 has an isoelectric point of about 4.7. This indicates a significant difference in surface functionality of the two membranes, though further characterization of the chemical differences was beyond the scope of this study. SW30HR is commercially coated with polyvinyl alcohol, which neutralizes many of the dangling carboxyl groups of the polyamide active layer and creates a more neutrally charged membrane over the pH range used in titrations (3 to 9).

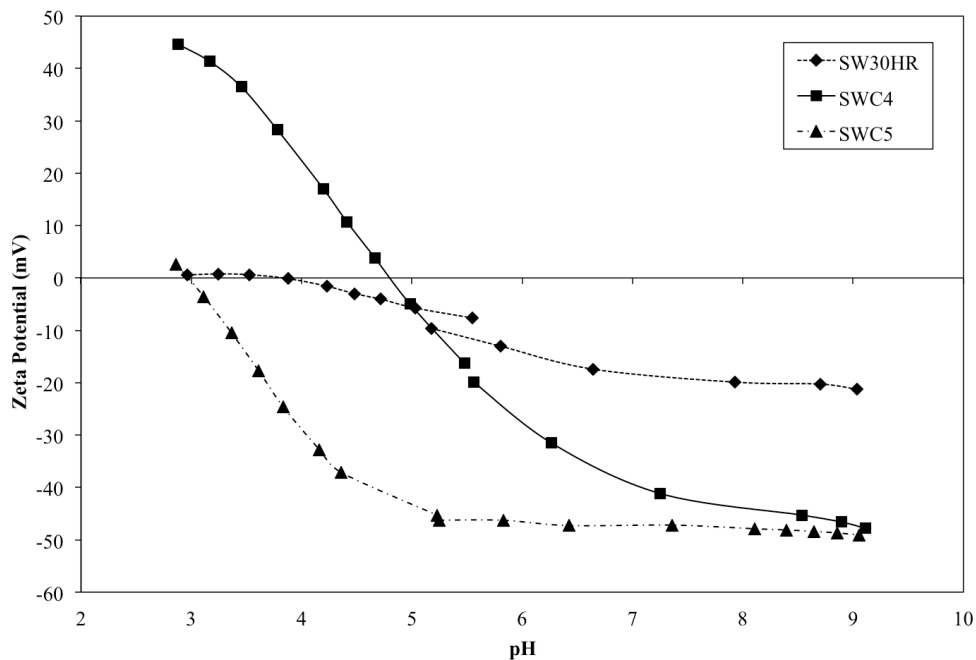


**Figure 3.6.** Zeta potential curves for SW30HR, SWC4 and SWC5 TFC PA membranes. Breaks in the titration curve resulted from the separation of acid and base titrations, which provided separate sets of data.

Some variability was noted between samples of the same membrane, demonstrated in Figure 3.7 by SW30HR samples. This was an expected result as surface layer heterogeneity is a well-reported property of commercially prepared RO membranes

(Coronell et al., 2011; Freger, 2003). From August 2011 onward, samples were cut from a dry membrane sheet and soaked in water overnight before analysis. Titration data from “old” membranes soaked for more than a month and “new” membranes soaked for less than a week suggest that contact time with water affects the membrane surface chemistry, with the surface becoming more negatively charged over time. SWC5 was purchased as a full membrane module that arrived pre-tested and vacuum-sealed in water, so it may be expected that the surface charge of SWC5 will not change as significantly as a function of water soaking time.

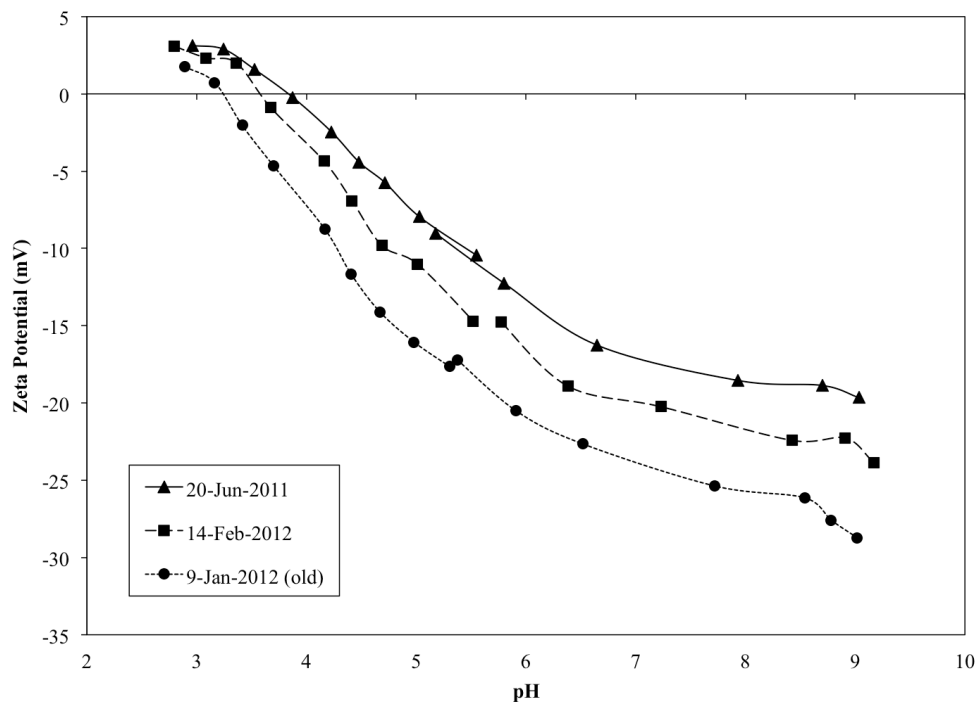


**Figure 3.7.** Titrations of three SW30HR samples. Titrations have very similar shapes but vary slightly in zeta potential, as seen with the June and February data. The January titration was performed after the membrane had been stored at 4°C for over 3 months.

When acid cleaning experiments were performed using SW30HR membrane, the zeta potential curve of SW30HR decreased significantly after washing in pH 1 solution

for 30 minutes (Figure 3.8). A significant decrease in zeta potential indicates that the surface chemistry was modified by the very low pH cleaning of the membrane. One possible change is that the polyvinyl alcohol layer may have been removed to some extent. This phenomenon was not observed with cleaning solutions of pH 3 or higher, as Figure 3.8 shows. The pH 1 cleaning appears to damage the coating layer of the SW30HR membrane and is compared to the uncoated PA of SWC5 in Figure 3.9 to determine whether the data provide a rough approximation of PVA removal. Similar experiments were outlined for SWC4 and/or SWC5 membrane, but have not been performed yet. Acid cleaning of SWC4 and SWC5 could confirm the hypothesis that PVA is somewhat removed by low pH cleaning, or could indicate another phenomenon entirely.

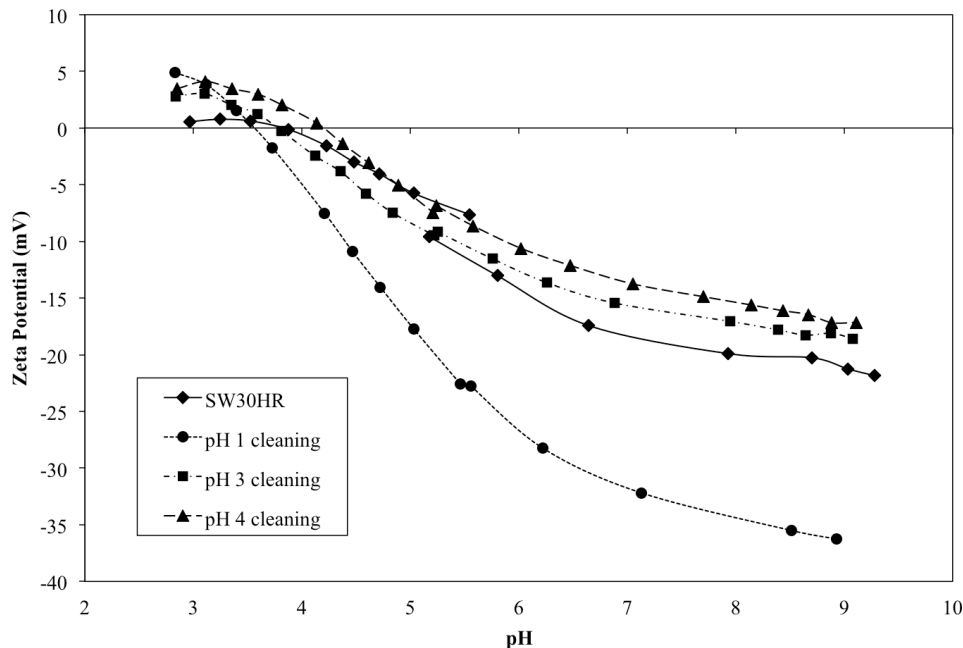


**Figure 3.8.** SW30HR samples in HCl solutions of varying strength for 30 min. Strong acid significantly altered the zeta potential while weaker acid solutions did not.

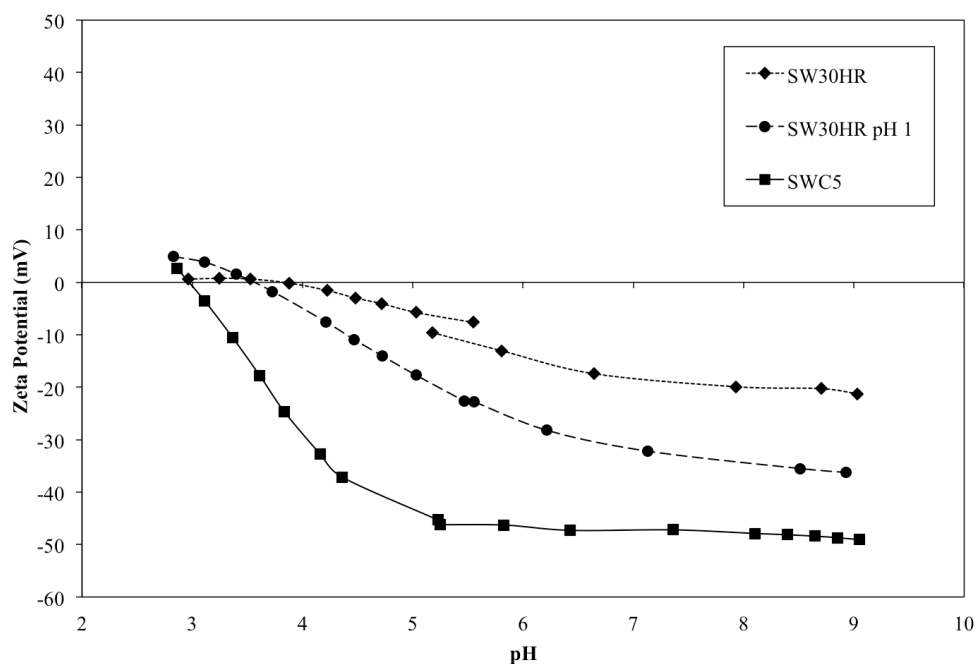


**Figure 3.9.** Zeta potential drop of pH 1 acid-washed SW30HR compared to virgin SW30HR and SWC5 membranes.

### 3.5 Polymer and nanoparticle characterization

PolyDADMAC and both TiO<sub>2</sub> NP stock solutions were prepared at the beginning of the project and lasted throughout the duration of the project. Silver NP stock solution was prepared twice over the course of the project. The first solution was not characterized, which exacerbated erroneous calculations of NP concentrations and misleading data in the preliminary results. Concentrations of NP solutions were not measured until the culmination of the project, an oversight that left many questions about multiple sets of data. Future work with this project should include characterization of stock solutions immediately after preparation and periodically thereafter to determine the extent to which nanoparticles degrade or aggregate over time.

### 3.5.1 *PolyDADMAC*

PolyDADMAC concentration of the hundredfold dilution was assumed to be 0.2% polymer in the aqueous working solution. This assumption was based on the hydrophilic properties of the polymer. Stock solution was measured into a graduated cylinder that was then rinsed several times into a volumetric flask to ensure complete transfer of the polymer during dilution. The method was significantly more reliable than using a pipette due to the viscous nature of the concentrated stock solution. PolyDADMAC is not UV active or fluorescent; manufacturers could not recommend a simple laboratory experiment to quantify polyDADMAC so reported concentrations are based on dilution volumes.

### 3.5.2 *Nanoparticle concentration determination using ICP-OES*

NP working solution concentrations were measured by ICP-OES using Aristar Plus multielement standard for trace metal analysis, which contained 10 mg/L Ag (BDH Ltd, Radnor, PA; lot C2-MEB296061). Excellent calibration curves were obtained for both materials, with an  $R^2$  value of 0.99991 for Ag calibration and 0.99946 for Ti calibration. Silver NPs were received in aqueous suspension and diluted into DDI water to make working solutions. Early use of a high concentration of Ag(-) NPs resulted in aggregation, which was observable on low-magnification SEM images. TiO<sub>2</sub> NP concentrations were prepared from powdered NPs diluted into DDI water. These NPs were observed adhered to glassware used for stock solution preparation, so not all of the material was fully dissolved into the stock solutions.

The 0.1 g/L silver NP working solution was first diluted by 50%, resulting in an expected concentration of 50 mg Ag/L. This sample concentration was far greater than the highest standard, so the 50 mg/L Ag samples were diluted by 100 for a final anticipated sample concentration of 0.5 mg Ag/L. A miscalculation regarding the final anticipated Ag concentration resulted in a calibration curve 10x lower than necessary. The calibration curve had a high  $R^2$  value despite being too low in concentration and was used for preliminary Ag concentration analysis. Based on the calibration curve and instrument response for Ag samples (Table 3.3), the NPs appear to have dissolved completely in 5% HNO<sub>3</sub>. ICP results indicate that Ag concentrations were 0.47±0.004 mg Ag/L, which was in excellent agreement with the expected 0.5 mg Ag/L.

**Table 3.2.** ICP data for Ag standards and triplicate working solution diluted to 0.5%.

Sample	Signal Intensity	[Ag]	Average [Ag]
Ag(-) 1	9911	0.46	0.47±0.004
Ag(-) 2	10077	0.47	
Ag(-) 3	10042	0.47	
Ag Std 0ppm	-76.13	0.00	N/A
Ag Std 0.01 ppm	120.04	0.01	
Ag Std 0.025ppm	449.09	0.025	
Ag Std 0.05ppm	1001.10	0.05	
Ag Std 0.1ppm	2078.54	0.10	

A 1 g/L titanium standard was used for calibration, allowing Ti NP stock solutions to be diluted 1:1 in 5% HNO<sub>3</sub>, with a final concentration of 2.5% HNO<sub>3</sub>, for ICP analysis. Concentrations were expected to be similar for the positive and negative NPs; stock solutions were calculated as 212 mg Ti/L and 184 mg Ti/L for TiO<sub>2</sub>(+) and TiO<sub>2</sub>(-), respectively. For the diluted solutions, ICP data were expected to yield approximately 100 mg/L for TiO<sub>2</sub>(+) and 90 mg/L for TiO<sub>2</sub>(-). However, ICP results indicated a concentration of 5.5 mg/L for TiO<sub>2</sub>(-) and 55 mg/L for TiO<sub>2</sub>(+) (Table 3.2).

Disagreement between expected values and ICP results was most likely caused by incomplete dissolution of TiO<sub>2</sub> NPs. An acid or microwave digestion would be needed to completely dissolve Ti NPs. Data suggest that TiO<sub>2</sub>(+) NPs are more soluble in HNO<sub>3</sub> than TiO<sub>2</sub>(-) NPs.

**Table 3.3.** ICP data for Ti standards and triplicate working solutions diluted to 50%.

Sample	Signal Intensity	[Ti] (mg/L)	Average [Ti] (mg/L)
TiO <sub>2</sub> (-) 1	286325	5.07	5.4±1.5
TiO <sub>2</sub> (-) 2	368288	6.96	
TiO <sub>2</sub> (-) 3	242744	4.06	
TiO <sub>2</sub> (+) 1	2525300	56.7	54.9±1.8
TiO <sub>2</sub> (+) 2	2441280	54.8	
TiO <sub>2</sub> (+) 3	2370068	53.1	
Ti Std 0ppm	101	0.0	N/A
Ti Std 10ppm	456409	10.0	
Ti Std 25 ppm	1150798	25.0	
Ti Std 100 ppm	4583184	100.0	
Ti Std 250 ppm	10836125	250.0	

## CHAPTER FOUR

### COATING CONDITION OPTIMIZATION

The goal of this chapter is to describe the conditions required for effectively coating RO membranes with NPs. Each coating material was prepared at several different concentrations and the effects were examined by electrokinetic measurements in the SurPASS. Once optimal concentrations were determined, coating times were varied to determine how quickly coatings would assemble. NP concentrations are reported as mass of the metal component (Ti or Ag) per liter, as the manufacturer did not provide more specific particle analysis. A mass-based measurement is insufficient to quantify NP concentration on the membrane as the number of metal atoms present per NP is unknown, but an alternative method of quantification has not yet been identified.

#### 4.1 Determining coating concentrations

##### 4.1.1 *PolyDADMAC coating layer*

PolyDADMAC was used as a positive binding layer bridging between negatively charged NPs and the negatively charged membrane surface. Coating solutions were prepared by dilution of the stock solution using DDI water. PolyDADMAC coatings of 5%, 2% and 0.2% (w/v) were applied to dry SWC4 membranes to test concentration effects on a highly negative membrane. Coatings of 2%, 1% and 0.2% were applied to dry SW30HR membrane after SWC4 data was collected. All coatings for the concentration experiments were allowed to assemble for 24 hours in the refrigerator (4°C). Membranes were removed from coating solution, rinsed in 200 mL DDI water for

30 seconds and stored in DDI water in the refrigerator for at least 12 hours before analysis or further coating.

During the process of determining coating concentrations, it was decided that using wet membranes would be more applicable to plant operating conditions, so the 0.2% coatings for negative NP experiments were assembled onto wet SW30HR membranes from August 2011 onward. Results of coating dry membranes with 0.2% polyDADMAC were compared to those for coating wet membranes with 0.2% polyDADMAC.

#### *4.1.2 TiO<sub>2</sub>(+) NPs on membrane surface*

TiO<sub>2</sub>(+) NPs were electrostatically adsorbed directly to the membrane surface. SWC4 was initially used for TiO<sub>2</sub>(+) concentration experiments because the surface carries a stronger negative charge. Carboxyl groups of the SWC4 surface are not shielded by polyvinyl alcohol coating as with the SW30HR membrane, resulting in a higher charge density. TiO<sub>2</sub>(+) coatings were prepared by diluting 10 µL and 20 µL of TiO<sub>2</sub>(+) stock solution into 10 mL, resulting in concentrations of 0.212 mg Ti/L and 0.423 mg Ti/L, respectively. Dry membrane coupons of SWC4 were submerged in the coating solution for 24 hours at 4°C. These concentrations did not alter surface charge, so for SW30HR experiments higher concentrations of 21.2 mg/L, 10.6 mg/L, 4.2 mg/L and 2.1 mg/L were used. Single measurements were taken to quickly determine the zeta potential changes imparted by varying the NP concentrations.

#### *4.1.3 Ag(-) NPs on polyDADMAC coated membranes*

Ag(-) NPs were adsorbed onto a 0.2% polyDADMAC binding layer. Initial experiments used concentrations of 100 mg Ag/L, 50 mg/L and 10 mg/L. PolyDADMAC-coated membrane coupons were placed into Ag(-) coating solutions after at least 12 hours in DDI water. After 24 hours, Ag(-) coated membranes were rinsed for 30 seconds and soaked in DDI water at least overnight before analysis. Soaking allowed detachment of any NPs not adsorbed to the membrane.

#### *4.1.4 TiO<sub>2</sub>(-) NPs on polyDADMAC coated membranes*

TiO<sub>2</sub>(-) NPs were adsorbed onto a 0.2% polyDADMAC binding layer. Initial experiments used 18.4 mg Ti/L, 9.2 mg/L and 1.8 mg/L. As with Ag(-) NPs, polyDADMAC coated membrane coupons were coated with NP coating solution at least 12 hours after polyDADMAC coating. Samples were coated with TiO<sub>2</sub>(-) for 24 hours, then rinsed for 30 seconds before soaking in DDI water at 4°C at least overnight.

#### *4.1.5 Coating controls*

Coating controls were prepared to confirm that binding of the coating layers was electrostatic. Controls included TiO<sub>2</sub>(+) exposed to a polyDADMAC coated membrane, TiO<sub>2</sub>(-) exposed to a virgin membrane and Ag(-) exposed to a virgin membrane. NPs were not expected to bind in control experiments due to electrostatic repulsion.

## **4.2 Coating concentration results**

### *4.2.1 PolyDADMAC coatings*

PolyDADMAC coatings adsorbed strongly to the PA membranes, causing a significant increase in zeta potential (Figure 4.1). The polyDADMAC coating resulted in

a positive zeta potential over the entire pH range of the titration (3 to 9). The increase in zeta potential at the low end of the pH range can be attributed to high proton density at the membrane surface.

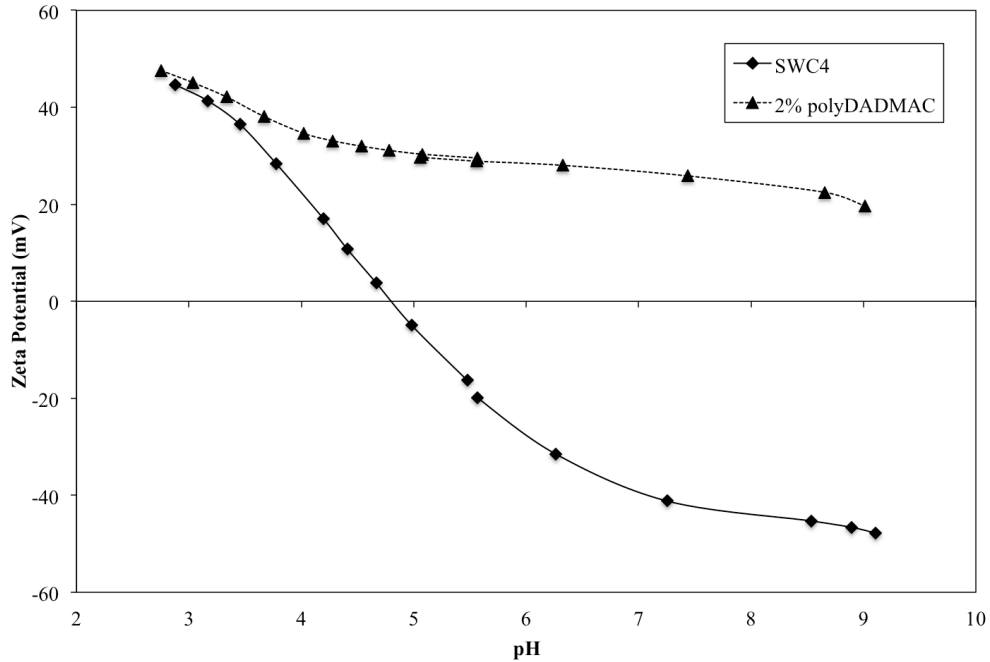


**Figure 4.1.** PolyDADMAC coating on SWC4 membrane. The polymer coating significantly altered the surface chemistry, creating a positively charged membrane surface.

Varying concentrations of polyDADMAC were applied to SW30HR membranes to determine a threshold concentration. The lowest effective coating concentration was desired to keep polyDADMAC coatings thin. Figure 4.2 shows zeta potential titrations for concentrations of 2%, 1% and 0.2% on dry-coated SW30HR membranes. All concentrations produced a significant increase in zeta potential, with a negligible difference between 0.2% and 1% concentrations and only slightly higher zeta potential for 2% concentrations. The 0.2% concentration was selected for further experiments because of the effectiveness at a low concentration.

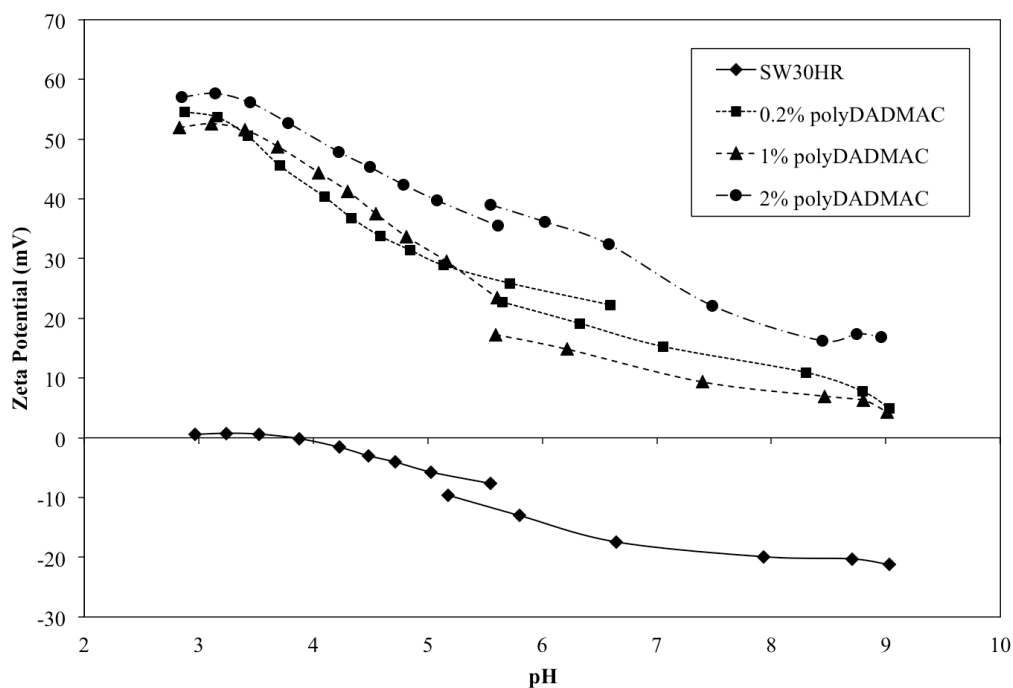


**Figure 4.2.** PolyDADMAC coatings of 2%, 1% and 0.2% on dry SW30HR membranes. All coatings impart a strong charge; there is no notable difference between 0.2% and 1%, and little difference at 2%.

#### 4.2.2 $TiO_2(+)$ NP coatings

$TiO_2(+)$  NPs, which were functionalized by the manufacturer with polyDADMAC, adsorbed directly to PA membranes, changing the surface charge from negative to positive. The zeta potential did not change when 0.212 mg/L and 0.424 mg/L of  $TiO_2(+)$  was applied to SWC4 membranes. Higher concentrations were applied to SW30HR membrane and did change the surface charge, indicated by changes in single measurement values in Figure 4.3. The 21.2 mg/L  $TiO_2(+)$  solution imparted the smallest change and had the tightest error bars. Error bars in Figure 4.3 suggest that the instrument may not be sensitive enough to accurately evaluate small changes in zeta potential incurred from varying NP concentrations. The 4.2 mg Ti/L coating was selected for future work because of the relatively high zeta potential and low concentration.

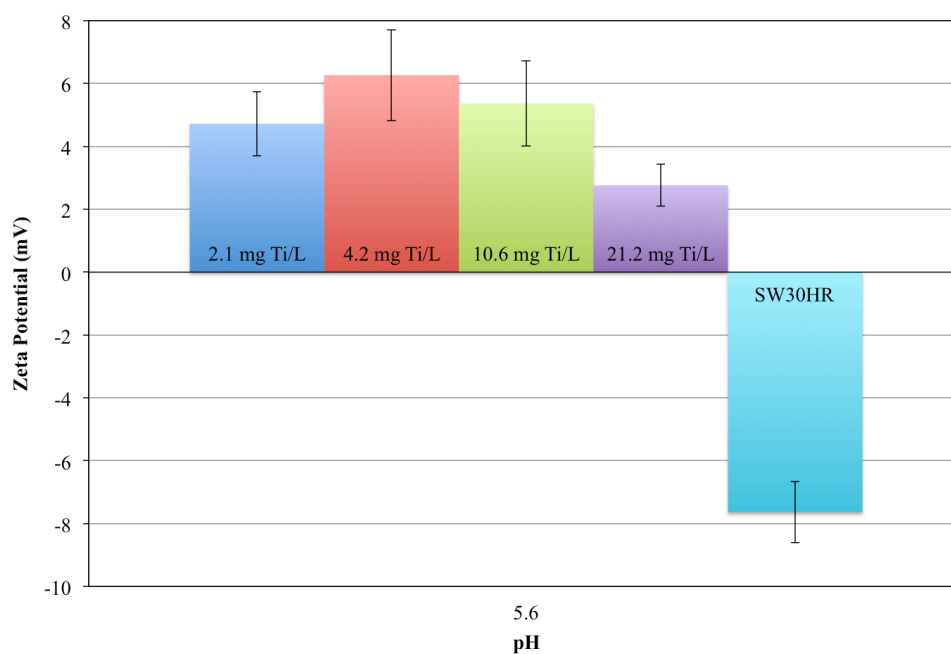


**Figure 4.3.** Effects of 2.1 mg/L, 4.2 mg/L, 10.6 mg/L and 21.2 mg/L TiO<sub>2</sub>(+) on membrane surface charge compared to the uncoated SW30HR membrane. Error bars represent a standard deviation from 12 measurements.

The TiO<sub>2</sub>(+) coatings varied quite significantly between experiments. A set of experiments was prepared in August 2011 and a second set was prepared in May 2012. The difference in titration curve between the two TiO<sub>2</sub>(+) coated membranes was notable. The difference may be attributed to heterogeneity between membrane samples or NP aggregation over the course of the stock solution lifetime. Membrane heterogeneity seems unlikely, as virgin membrane comparisons did not vary nearly as much as the TiO<sub>2</sub>(+) coated membranes. If aggregation occurred in the stock solution, considerably different quantities of NPs could be acquired with each aliquot removed from solution and the coatings would not be uniform. The changes observed in Figure 4.4 suggest that NP stock solutions need to be buffered, sonicated or otherwise modified in the future to prevent aggregation. The manufacturer provided particle size analysis for the powdered

form of the NP that was received, but size analysis for the stock solution would be useful for detecting NP aggregates.

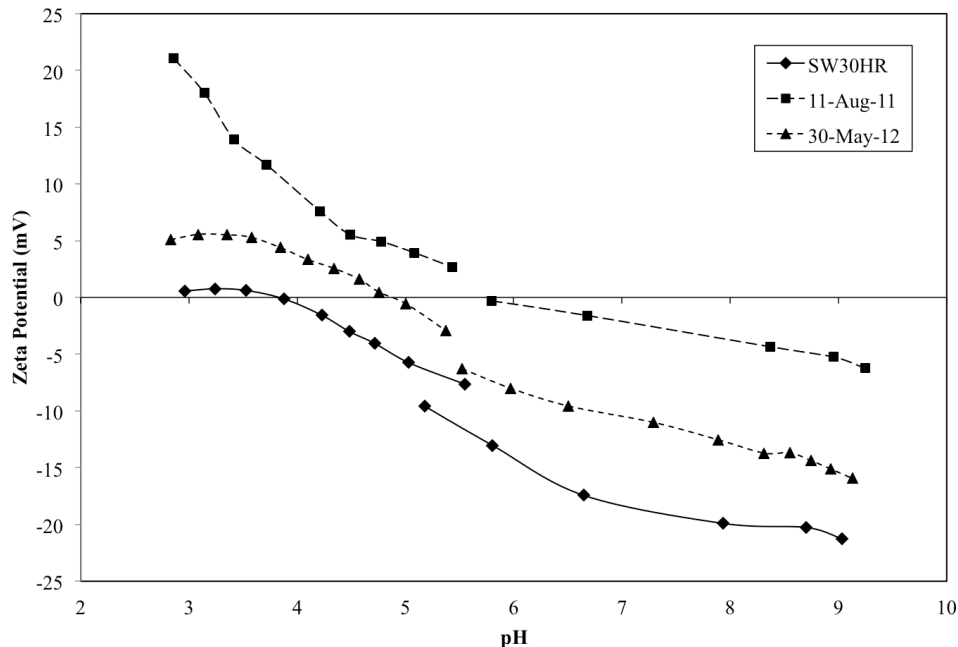


**Figure 4.4.** TiO<sub>2</sub>(+) NP coatings for two sets of experiments. Significant differences could be attributed to changes in NP stock solution or heterogeneity of the membrane surface.

Because TiO<sub>2</sub>(+) NPs were functionalized by polyDADMAC, it was initially expected that the NPs would impart a surface charge comparable to that of the linear polymer. Coating with NPs resulted in a significantly lesser positive charge, indicating a lower charge density (Figure 4.5). Upon further consideration it was concluded that the NPs could not impart a surface charge comparable to the polyDADMAC coating because each polymer chain included loops and tails that contributed significantly to the surface charge. Each NP, however, was a roughly spherical particle contributing a single point charge and resulting in a lower charge density. Surface packing may also have factored

in, with adsorption of the dilute polymer being a more highly favored mechanism than the aggregation of NPs at the membrane surface.

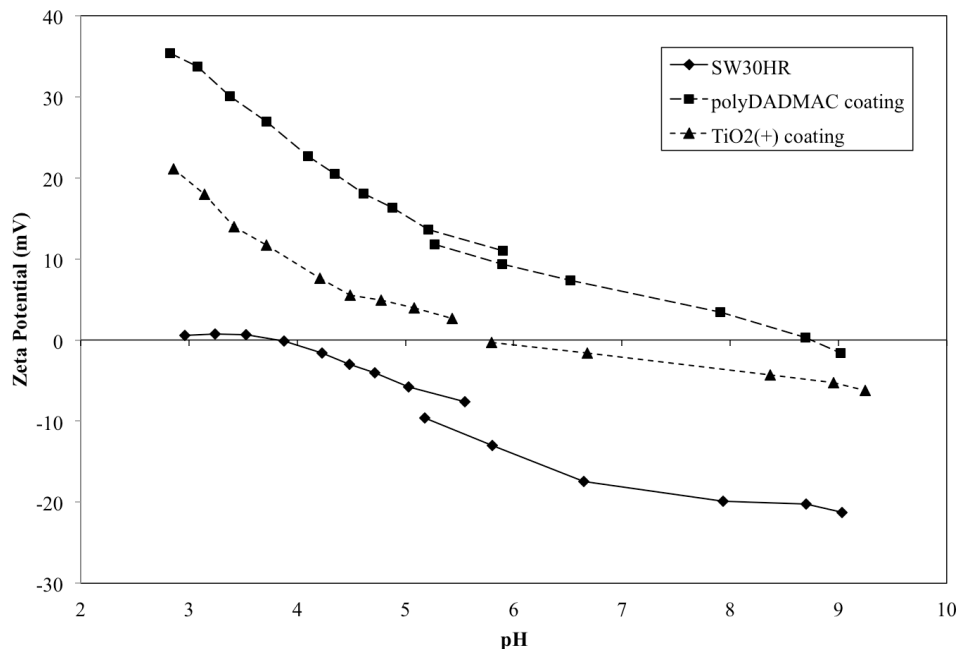


**Figure 4.5.** Charge density of polyDADMAC coating compared to TiO<sub>2</sub>(+) NP coating, which was functionalized with polyDADMAC.

#### 4.2.3 Ag(-) NP coatings

Ag(-) NPs, given negative charge by polyacrylate, adsorbed to the polyDADMAC-modified membranes. Adsorption was indicated by a decrease in the zeta potential of polyDADMAC coating. Ag(-) coating successfully reduced the strong positive charge of the polyDADMAC-coated membrane, bringing the zeta potential at pH 5.6 from +26 mV to a range of  $-1.5 \rightarrow +5$  mV (Figure 4.6). As expected, the higher concentrations of NPs resulted in a larger charge difference, with the 10 mg Ag/L coating maintaining a slightly positive surface charge and the 20 mg/L, 50 mg/L and 100 mg/L coatings imparting neutral to very slightly negative surface charges. Similarly to the

TiO<sub>2</sub>(+) data, the standard deviation of the zeta potential in Figure 4.5 exceeded the differences between most single measurement values for Ag(-) concentrations. The measurement with the highest standard deviation - 20 mg/L Ag(-) solution - was a data point from a titration curve, which was averaged from four measurements, while the other values were single measurement data that were averaged from 12 measurements. This indicates that the instrument is more precise when more measurements are used to report each data point. When 10 mg/L, 50 mg/L and 100 mg/L were compared, 100 mg/L coating solution was selected for future experiments because of its large zeta potential change. After NP aggregates were discovered, however, the concentration was reduced to 20 mg/L.

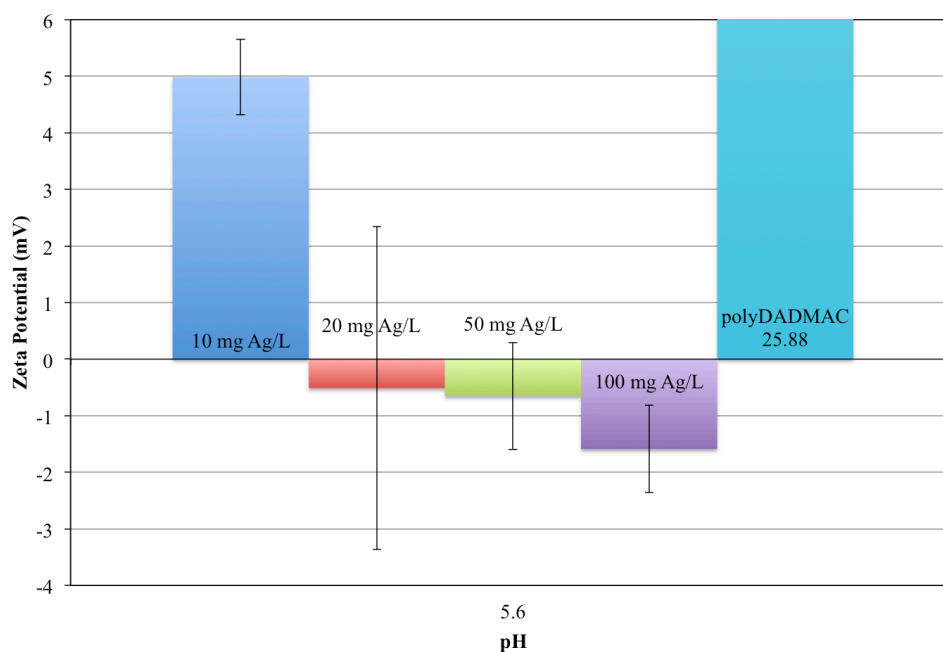


**Figure 4.6.** Reduction in surface charge by Ag(-) NPs adsorbed to polyDADMAC. As expected, the higher the NP concentration, the lower the zeta potential.

Titrations of Ag(-) NP coatings showed less deviation between individual titration than deviation between TiO<sub>2</sub>(+)-coated membranes. Membranes prepared at different times had agreeable acid titration curves from pH 4-6 (Figure 4.7). The shape of the base titration curves agreed as well, but the zeta potential of one sample dropped substantially between the acid and base titrations. This occurred because the experiment was left overnight before the base titration was run, allowing time for the acidic solution to remove some of the coating from the membrane. Had the second titration been run immediately after the first, the base titrations should have lined up almost exactly as observed in other titrations. Zeta potential was also measured for an Ag(-) coated membrane that had been stored for four months. The surface charge of the old membrane was considerably lower than both the fresh Ag(-) coated membranes and the uncoated SW30HR. This could be a result of the NPs dissolving, detaching from the membrane, or being otherwise altered by the storage solution (pH ~5.5). Biological growth would result in a decrease in surface charge, though the biocidal properties of nanosilver may mitigate such fouling. The mechanism for zeta potential decrease after long-term storage has not yet been identified.

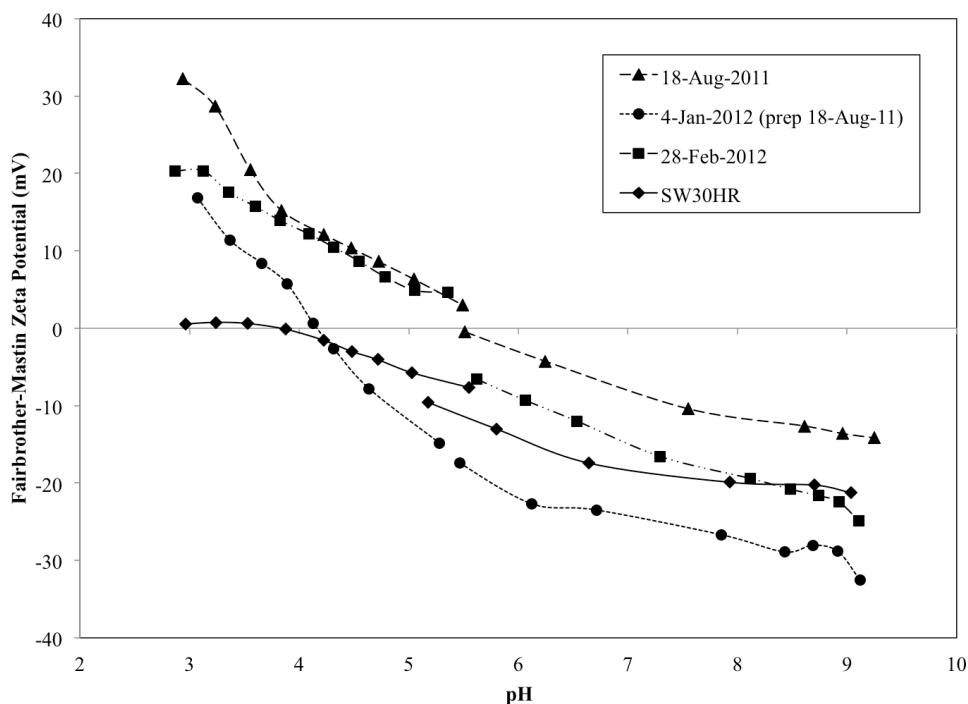


**Figure 4.7.** 20 mg/L Ag(-) coatings compared to virgin SW30HR.

SEM analysis of membranes revealed aggregation of the Ag(-) NPs in low magnification (2,500 magnification) images (Figure 4.8). Aggregates of up to 6  $\mu\text{m}$  were visible. The size is considerable when compared to the 10nm nanoparticles. Based on SEM images, the higher charge density on the 100 mg/L Ag(-) surface was attributed to aggregates rather than more NPs providing better coverage of the membrane surface. A “breakthrough” aggregation concentration likely occurs between 50-100 mg/L; there is little difference between surface charge of the 20 mg/L and 50 mg/L coatings, indicating the coatings may be similar in NP density, while aggregates form on membranes coated with 100 mg/L Ag(-) NPs. The concentration used for coatings was decreased to 20 mg Ag/L to decrease likelihood of aggregation and obtain data that could be compared to  $\text{TiO}_2(-)$  coatings.

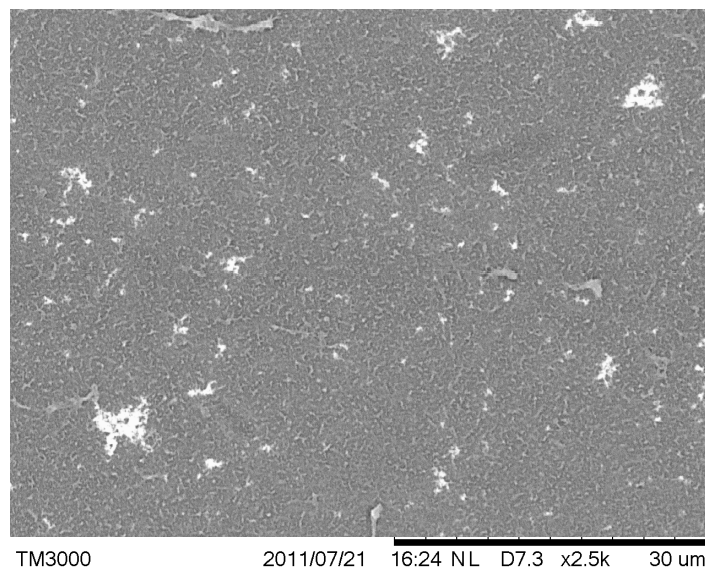


**Figure 4.8.** SEM image of Ag(-) aggregation on SW30HR membrane. Aggregates are very large, up to 6 $\mu$ m in size. Nanoparticles are ~10nm.

#### 4.2.4 $TiO_2(-)$ NP coatings

$TiO_2(-)$  NPs, given negative charge by polyacrylate, adsorbed to the polyDADMAC-coated membranes. Adsorption was indicated by a decrease in the zeta potential of the polyDADMAC coating (Figure 4.9).  $TiO_2(-)$  coating resulted in a similar degree of zeta potential change as the Ag(-) coating; however, the variation between individual  $TiO_2(-)$  coatings and individual Ag(-) coatings prevented the assumption that the different NPs provided equal coverage of the surface. Ag(-) experiments used 20 mg Ag/L while  $TiO_2(-)$  experiments used 4.2 mg Ti/L; assuming that the metal component per NP is comparable between Ti and Ag NPs, more Ag was used in experiments than Ti. The observed variation in zeta potential, imparted by the same coating solution in different experiments, could be attributed to charge density heterogeneity of the polyDADMAC layer, heterogeneity of the virgin membrane, aggregation or charge density heterogeneity of the NP coatings, or a combination. Uneven polyDADMAC or

NP coatings are more likely than significant membrane heterogeneity. TiO<sub>2</sub> NPs may have aggregated as the stock solution aged, causing large clusters of NPs to adsorb to the membrane surface; particle size analysis of the stock solution would allow this possibility to be confirmed or eliminated. TiO<sub>2</sub>(-) was not visible in SEM images at the time the Ag(-) aggregates were discovered, so further SEM imaging was not pursued for TiO<sub>2</sub>(-) coatings.

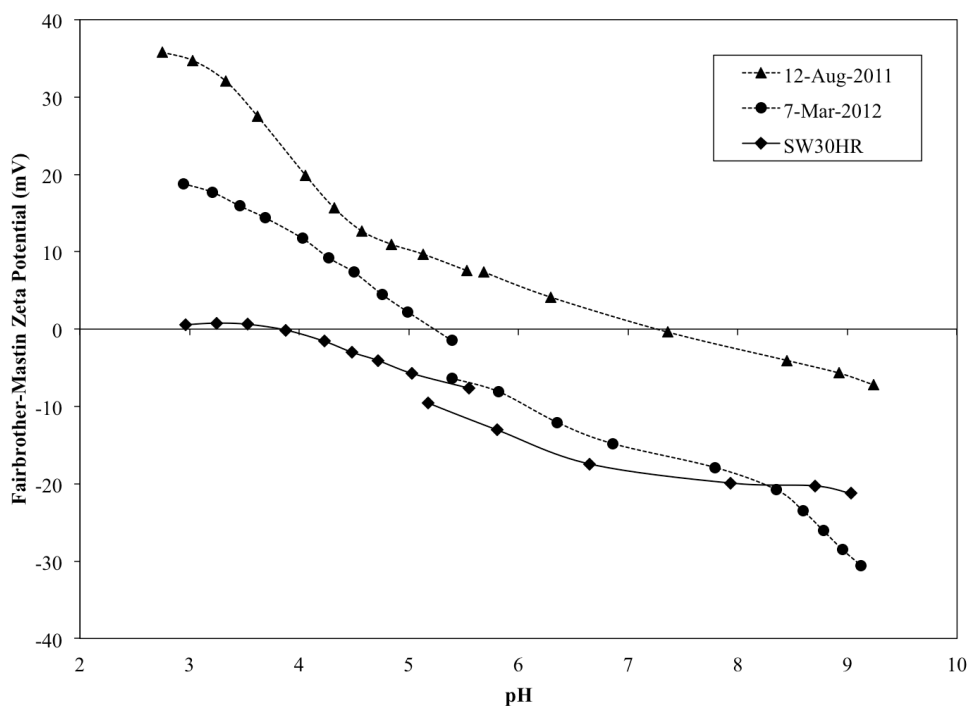


**Figure 4.9.** TiO<sub>2</sub>(-) coatings on polyDADMAC membranes from two experiments. Deviation in shape and zeta potential were observed.

### 4.3 Membrane coating methods

Coatings were self-assembled onto the membranes in 10 mL polypropylene petri dishes, which allowed membrane coupons to float easily in coating solution. Two membrane coupons of approximately 1.5 cm x 2.5 cm were coated in each dish. One

membrane was placed active side up and one active side down to prevent the coupons from sticking together and interfering with coatings. Despite different orientation, both membranes were completely submerged during the entire coating process.

Membrane coupons for initial experiments, particularly concentration studies, were coated in the refrigerator (4°C) to prevent photodegradation of the membrane samples and inhibit any biological growth. As method development progressed, it was decided that room temperature coating processes better simulated real world conditions and that photodegradation and biological growth were not a concern on experimental time scales of less than 24 hours. To emulate movement across the membrane surface similar to the flushing of feed water through modules in a RO plant, a rocker table was used on the bench top at room temperature (22±2°C) for coatings used in removal (Chapter 5) and RO (Chapter 6) experiments. Coating (Chapter 4) experiments from August 2011 also utilized the rocker table.

#### **4.4 Coating method evaluation**

##### *4.4.1 Wet vs. dry membranes*

For the concentration experiments, dry membrane coupons were placed into polyDADMAC or TiO<sub>2</sub>(+) solution for coating. This caused inconsistency in coating conditions as the negative nanoparticles were applied to a wet membrane while the polyDADMAC layer and positive NP were applied to a dry membrane. It was determined that all coatings should be applied to wet membranes to emulate real-world conditions where possible. Figure 4.10 shows that polyDADMAC binding was stronger on a dry membrane than on a wet one, but this effect could also be attributed to whether the

coating process was dynamic (wet membrane), allowing less loose binding, or binding via passive adsorption in a static solution (dry membrane). The stronger affinity of polyDADMAC for the dry membrane is assumed to be a result of static vs. dynamic coating conditions rather than temperature or degree of membrane saturation. Coating a wet membrane in cool, static conditions could easily test this hypothesis.

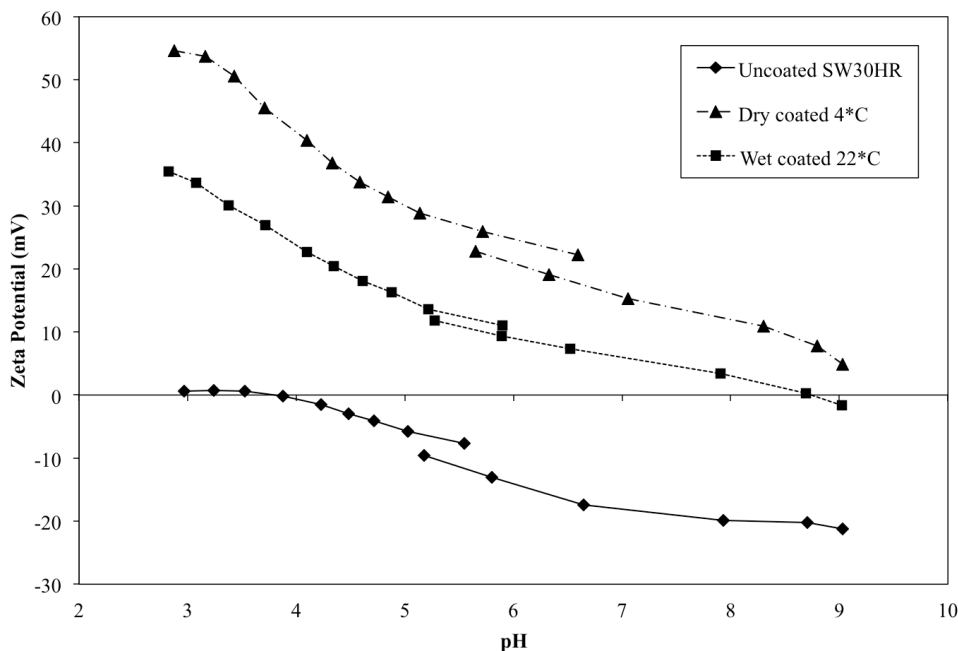


**Figure 4.10.** Titrations for polyDADMAC-coated SW30HR show that a dry membrane coated statically at low temperature had a more positive charge than a wet membrane coated dynamically at room temperature.

#### 4.4.2 Control coatings

Control experiments were performed to determine whether coatings adsorbed via electrostatic interactions alone or a combination of factors (H-bonding, van der Waals forces, etc.).  $\text{TiO}_2(+)$  did not alter the zeta potential or curve shape of the polyDADMAC-coated membrane (Figure 4.11), indicating that positive NPs did not adsorb to the polymer coating layer.  $\text{Ag}(-)$  and  $\text{TiO}_2(-)$  NPs adsorbed almost equally to the bare

SW30HR membrane despite electrostatically-repelling carboxyl groups present in both the NPs and membrane surface. Atop the PA layer SW30HR had a commercially applied layer of uncharged PVA, which served as a barrier between the membrane carboxyl groups and the negatively charged NPs and allowed adsorption to the membrane surface via non-electrostatic interactions, such as van der Waals forces. Negative NPs would be expected to show less affinity for SWC4 and SWC5, both of which are bare PA and have significantly stronger negative character than SW30HR. Experiments with SWC4 and SWC5 were laid out but not performed, so future work may confirm or deny this hypothesis. It was assumed that the polyDADMAC binding layer carried strong enough charge to attract the negative NPs and overpower alternate adsorption pathways.

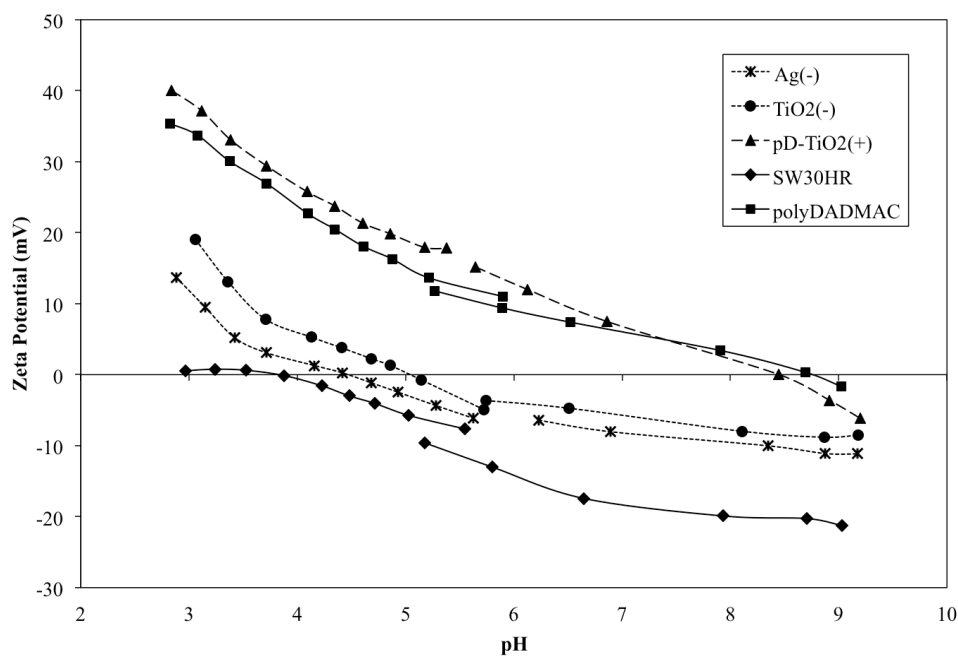


**Figure 4.11.** Control coatings on SW30HR. TiO<sub>2</sub>(+) did not adsorb to polyDADMAC; TiO<sub>2</sub>(-) and Ag(-) appear to have adsorbed to SW30HR despite carboxyl groups promoting electrostatic repulsion.

#### 4.4.3 SEM imaging results

SEM was used to investigate whether applied coatings were thick enough to be visible on the membrane surface. Initial SEM analysis after coating experiments used the TM3000 instrument with a maximum resolution of 10,000 (10k) magnification. Even with relatively low magnification of 2.5k, Ag(-) aggregates of up to 6  $\mu\text{m}$  were visible on the membrane surface when coated with 100 mg Ag/L NP solution (Figure 4.7). Titanium NPs, applied in much lower concentrations, were not visible on the membrane surface (Figure A.1). A higher resolution instrument, the SU6600, was used to achieve 100k magnification of the membrane surface. Ag(-) coatings of 20 mg Ag/L were used for the high resolution imaging but were not visible on the membrane surface at the lower concentration (Figure A.2). PolyDADMAC coatings, not visible at 10k magnification, were visible in 100k images as “filled in” valleys in the membrane structure (Figure 4.12).

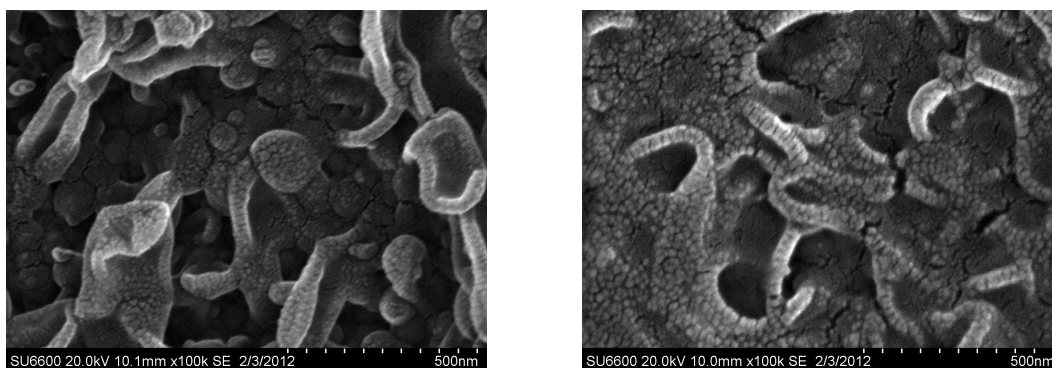


**Figure 4.12.** SEM images of virgin SW30HR (left) and polyDADMAC-coated SW30HR (right). PolyDADMAC coating appeared to fill in the loop and valley structure of the membrane.

#### 4.4.4 ATR-FTIR analysis

Infrared spectroscopy was used to investigate whether coatings were present in sufficient quantities to impart changes in infrared spectra. A significant quantity of polyDADMAC coating was expected to result in an emerging C-N peak at  $\sim 1100\text{ cm}^{-1}$ , while polyacrylate from the negative NP coatings was expected to result in a shift of the carboxyl C=O as the aliphatic carboxyl group contributed to the peak. However, no changes were observed in the presence of any coating (Figure 4.13), substantiating the conclusion that coatings were thin.

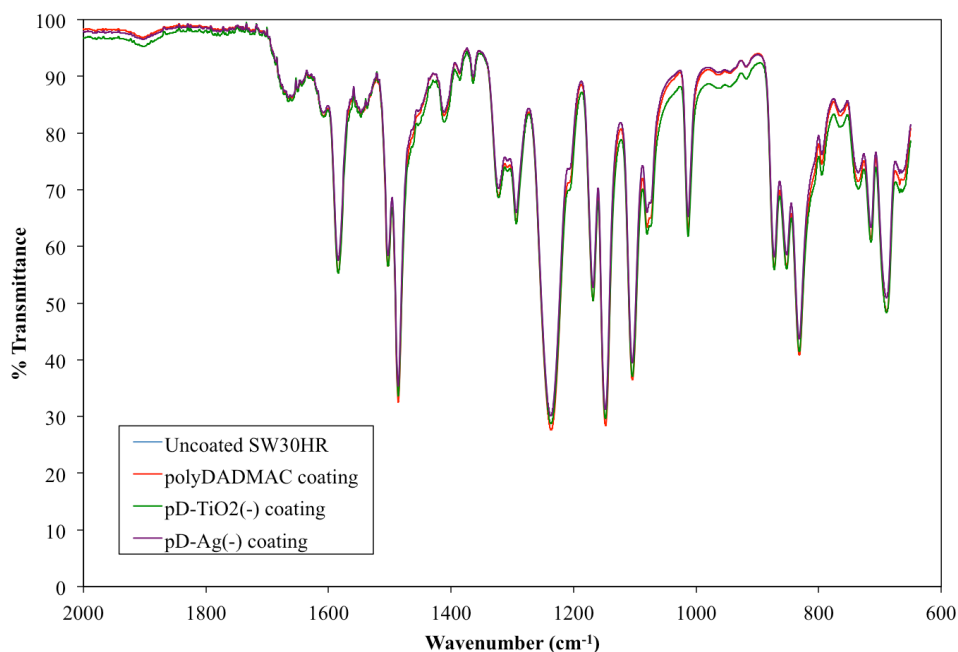


**Figure 4.13.** ATR-FTIR of polyDADMAC and negatively charged NP coatings did not indicate any changes in surface chemistry.

## CHAPTER FIVE

### REMOVAL OF COATINGS

One hypothesis of this work is that electrostatic interactions are the dominant mechanism for coating attachment, so simple acid or base cleaning should be sufficient for coating removal.

#### 5.1 Coating removal methods

For removal experiments, wet membranes were coated in 0.2% polyDADMAC solution on a rocker table at room temperature for 24 hr, soaked in DDI overnight and coated in NP solutions under the same conditions for 2 hr; TiO<sub>2</sub>(+) NPs were simply coated for 2 hr on the rocker table. Concentrations used for coating were 20 mg Ag/L Ag(-), 3.7 mg Ti/L TiO<sub>2</sub>(-) and 4.2 mg Ti/L TiO<sub>2</sub>(+). All coated membranes were soaked in DDI water for at least 12 hours before analysis or further coating to allow dissociation of any material not strongly attached to the membrane surface.

Coated membranes were exposed to hydrochloric acid (HCl) or sodium hydroxide (NaOH) solutions to investigate the appropriate conditions for coating removal. Initial removal experiments used strong HCl (pH 1) and NaOH (pH 13) for several hours. Membrane integrity limitations were addressed for subsequent experiments and acid solutions of pH 1, 2, 3 and 4 (HCl concentration 0.1, 0.01, 0.001 and 0.0001 M) were used for no longer than 30 minutes as per manufacturer recommendations. Control samples of virgin membrane were washed at each acid and base concentration to determine whether the caustic solutions altered the properties of the membrane (Figure 3.8). Strong cleaning with pH 1 HCl significantly altered the membrane, so

polyDADMAC and NP coatings were cleaned with pH 2, 3 and 4 solutions for the majority of experiments.

## **5.2 Coating removal results**

### *5.2.1 PolyDADMAC coating removal*

PolyDADMAC was effectively removed from the SW30HR membrane surface at a pH below the membrane isoelectric point (pH ~4 for SW30HR). As the pH decreased the membrane zeta potential became slightly positive, causing electrostatically unfavorable conditions for the polyDADMAC coating. Theoretically, as the membrane zeta potential increased, the polyDADMAC would be electrostatically repelled from the membrane and the coating removed. Figure 5.1 indicates that some polyDADMAC remained on the surface after cleaning with both pH 1 and pH 4 solutions. This was expected because of the nature of the polyDADMAC polymer. A highly charged, 80-120 kiloDalton (kDa) linear polymer, polyDADMAC likely bound to the PA surface at multiple contact points, creating a strongly bound coating layer. Removal of a single polyDADMAC chain would require every contact point to be electrostatically unfavorable; it is likely that a percentage of the polymer remained attached to the membrane at one or several contact points per chain.

SW30HR was used for coating removal experiments because it was not highly charged at low pH values, probably because of the PVA layer (as opposed to other membranes that do not have such a layer). Had the membrane been more positively charged at low pH, electrostatic repulsion between it and polyDADMAC would likely have been stronger, leading to greater removal. Since polyDADMAC was only used as a

binding layer for negative NPs, it was not considered a negative result for residual polymer to remain on the membrane. If applied in a membrane system, the polyDADMAC layer would be replenished anyway.

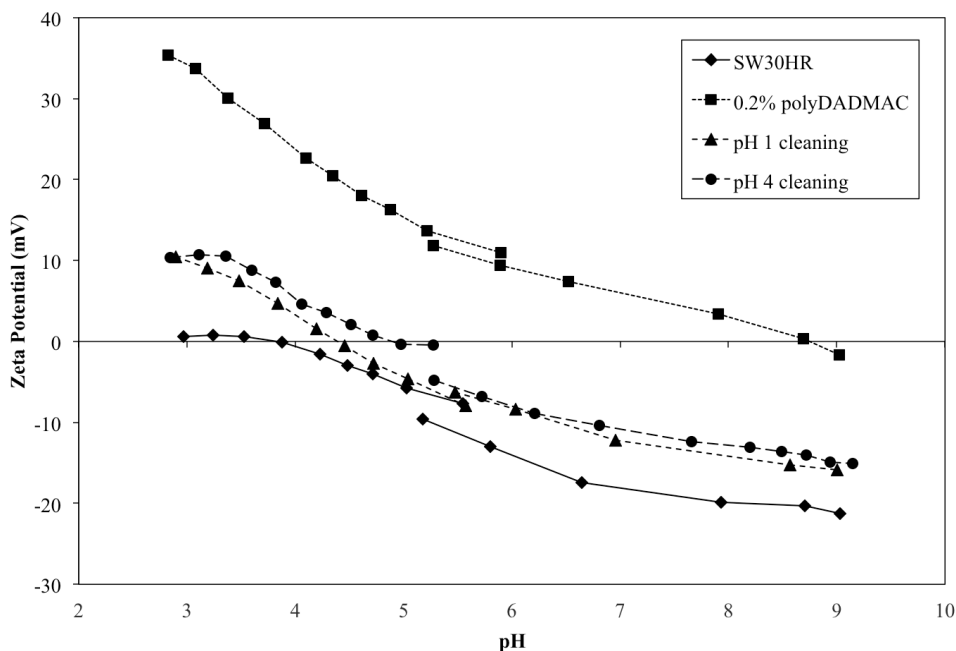


**Figure 5.1.** Acid cleaning of polyDADMAC-coated SW30HR resulted in significant but incomplete removal of the polymer.

PolyDADMAC was also subjected to a NaOH cleaning solution of pH 13 for 8 hours. Though the cleaning conditions exceeded the manufacturer recommendations for exposure time to high pH, some insights were gained from the single measurement data collected (Table 5.1). While the polyDADMAC-coated membrane had a zeta potential of +14 mV and the negative zeta potential of an acid-cleaned sample indicated some removal of the polyDADMAC layer, the base-cleaned sample retained a positive zeta potential of +8 mV. It is unclear from the experiments performed whether the decrease in zeta potential was caused by damage to the membrane by the caustic solution over an

excessive duration or if some of the polyDADMAC coating was removed. If the membrane was not damaged by caustic cleaning, polyDADMAC would be expected to adsorb more strongly to the membrane as the percentage of negative binding sites increased. The data may support this hypothesis: if a polyDADMAC chain adsorbed to the SW30HR surface at several points and the rest remained dangling from the surface, a high zeta potential would result. If the membrane became more negatively charged at high pH and the polymer chain became more attracted to the surface, the zeta potential measurement would decrease as the membrane neutralized a higher percentage of the polymer chain.

**Table 5.1.** Comparison of single measurement electrokinetic data for coating materials. Change in zeta potential for acid and base cleaning is reported as the difference between the coated membrane and after cleaning.

Sample	polyDADMAC ZP (mV)	Ag ZP (mV)	TiO <sub>2</sub> (-) ZP (mV)
Uncoated SW30HR	-12.8	-12.8	-12.8
pD or pD-NP coating	14.0	-2.3	5.5
pH 1 cleaning	-0.92	-11.8	-6.9
Change in ZP (acid)	-14.92	-9.5	-12.4
pH 13 cleaning	7.8	1.6	9.3
Change in ZP (base)	-6.2	3.9	3.8

### 5.2.2 TiO<sub>2</sub>(+) coating removal

TiO<sub>2</sub>(+) NPs were effectively removed by each acid concentration considered (Figure 5.2). Slight differences between titrations were assumed to be instrument variability rather than significant results since the pH 1 cleaning solution appears to have the highest zeta potential when compared to pH 2 and 3 cleaning solutions. When the titration curves of the acid cleaned membrane were compared to the virgin membrane, all of the NP coating appeared to be removed by acid solutions as weak as pH 3. NPs should

be roughly spherical in shape; if this was true,  $\text{TiO}_2(+)$  NPs adsorbed to the membrane surface via a single contact point and were simpler to repel or release from the membrane than was the polyDADMAC polymer. Base cleaning was not investigated for  $\text{TiO}_2(+)$  NPs based on the results of polyDADMAC-coated membrane cleaning; it was not anticipated to be an effective means of removing the positively-charged materials.

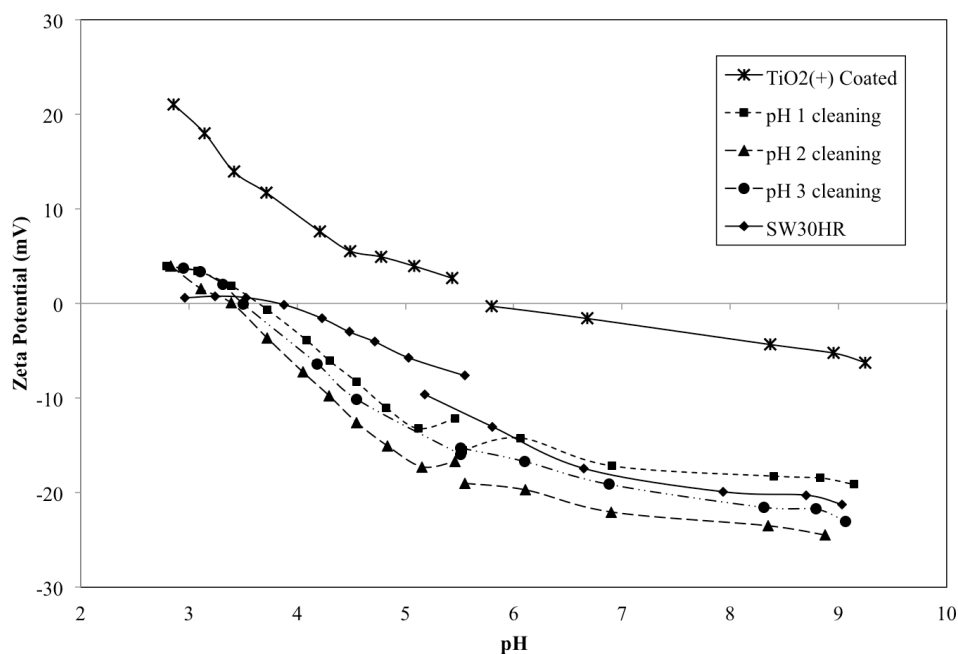


**Figure 5.2.** Acid cleaning of  $\text{TiO}_2(+)$  coatings. Acid cleaning resulted in complete removal of NPs for all acid concentrations investigated.

### 5.2.3 *Ag(-) coating removal*

Aggregation of  $\text{Ag}(-)$  NPs discovered by SEM imaging became an asset for coating removal data. Along with coatings, acid cleaning with pH 1 and base cleaning with pH 13 were observed using the TM3000 SEM (Figure 5.3). Aggregates were observed on the coated membrane as discussed previously. Fewer aggregates were observed on the acid-cleaned membrane, but some smaller aggregates remained. No

aggregates were located on the base-cleaned membrane. When considered along with electrokinetic data for samples from the same membrane coupons (Table 5.1), several conclusions can be drawn. The absence of NPs in the SEM image and increase in zeta potential indicate removal of the NPs and endurance of the polyDADMAC coating. Acid cleaning resulted in a significant drop in zeta potential, indicating removal of polyDADMAC coating but Ag(-) aggregates were still visible in SEM images. Two possibilities exist: either Ag(-) NPs adsorbed to the membrane surface via non-electrostatic interactions or aggregates remained adsorbed to the polyDADMAC polymer not removed from the membrane by cleaning. Control experiments indicated that NPs had adsorbed to the membrane surface in the absence of the polyDADMAC binding layer, so either mechanism is possible.

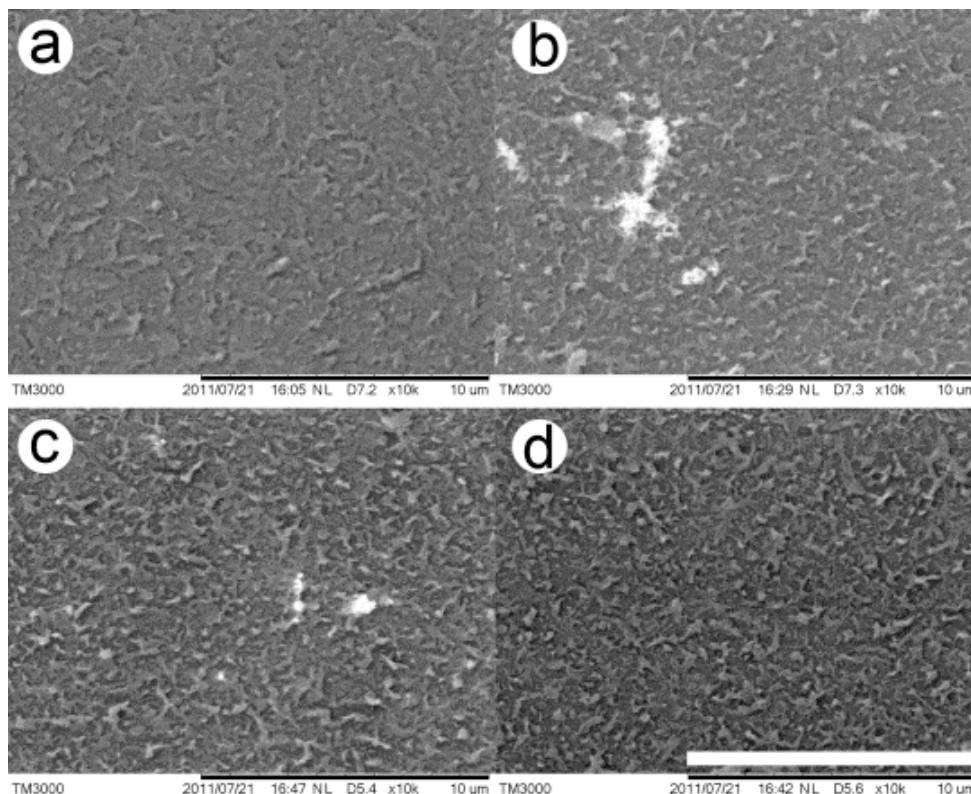


**Figure 5.3.** SEM images of uncoated SW30HR (a), Ag(-)-coated SW30HR (b), pH 1 acid-cleaned Ag(-)-coated SW30HR (c) and pH 13 base-cleaned Ag(-)-coated SW30HR (d).

Electrokinetic data were collected for titrations of acid-cleaned Ag(-)-coated membranes (Figure 5.4). An increase in zeta potential at the low end of the titration indicated that polyDADMAC remained on the membrane. The low zeta potential values at high pH drop below the SW30HR membrane, suggesting that NPs may remain adsorbed to the membrane and contribute to an increase in negative character at high pH.

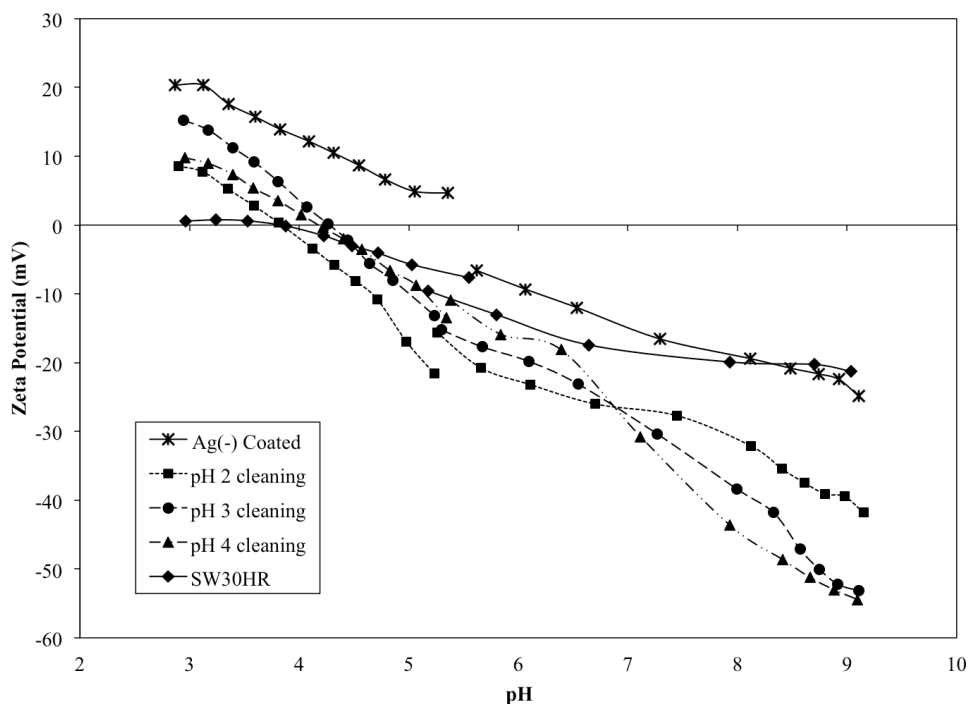


**Figure 5.4.** Electrokinetic behavior of Ag(-) coatings, bound to a polyDADMAC layer, after acid cleaning.

#### 5.2.4 $TiO_2(-)$ coating removal

$TiO_2(-)$  coatings behaved quite similarly to Ag(-) coatings for acid cleaning experiments. No NP aggregates were visible in SEM images because a low concentration (3.7 mg Ti/L) was used throughout the course of coating and removal experiments, but electrokinetic data were very similar to Ag(-) coatings, so similar conclusions regarding NP adsorption and detachment may be drawn. Single measurements for  $TiO_2(-)$  coating, acid and base titrations (Table 5.2) confirm the similar behavior to Ag(-). The  $TiO_2(-)$  coating imparted less charge decline because the concentration was much lower than that of Ag(-) (3.7 mg Ti/L vs 100 mg Ag/L). Acid cleaning resulted in a zeta potential drop while base cleaning resulted in an increase in zeta potential. When the quantitative change in zeta potential was compared for acid and base cleaning of Ag(-) and  $TiO_2(-)$

coatings, the results were very similar. These similarities suggested that the functionalizing polymer component of the composite NP (polyacrylate), rather than the inorganic component (Ti or Ag), contributed most significantly to NP behavior on the membrane surface.

Unlike with other coatings, electrokinetic behavior after acid cleaning of TiO<sub>2</sub>(-) coatings appeared to be directly related to acid strength (Figure 5.5). A pH 4 cleaning solution did not change the acid titration zeta potential values, and a drop in zeta potential for the base titration was attributed to leaving the membrane in acid overnight before running the second half of the titration. A pH 3 cleaning solution decreased the zeta potential slightly for both titrations. A pH 2 cleaning solution produced the largest change but still did not return the acid titration curve to the SW30HR values; the zeta potential remained high at low pH and dropped far below the SW30HR zeta potential during the base titration, indicating that NPs were still bound to the membrane and contributing additional negative charge at high pH.

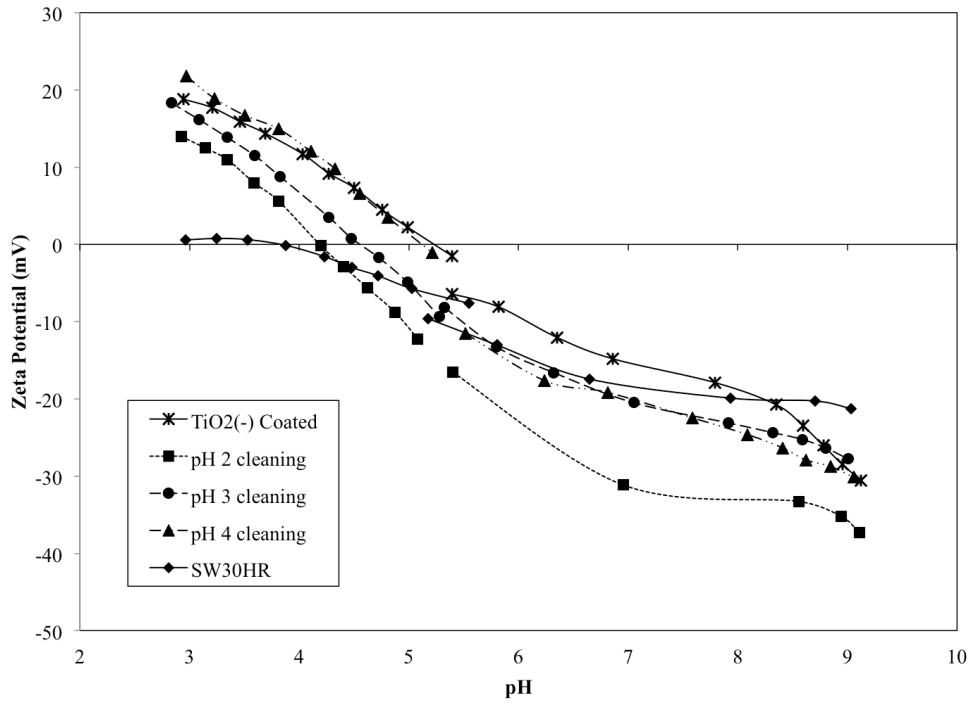


**Figure 5.5.** Electrokinetic behavior of TiO<sub>2</sub>(-) coatings after acid cleaning.

## **CHAPTER SIX**

### **BENCH SCALE REVERSE OSMOSIS FOULING EXPERIMENTS**

Bench scale reverse osmosis experiments were undertaken to begin testing the viability of the coating materials. Silver NPs were selected for bench scale RO experiments. Membranes coated for RO experiments were coated on the bench top as done previously. These experiments provide preliminary results for future work investigating fouling on RO membranes with removable coatings.

#### **6.1 Experimental design**

Three cycles of three experiments, outlined in Table 6.1, were performed in the bench-scale tests. The first cycle of experiments was performed with uncoated SWC5 membrane, the second cycle with polyDADMAC coated SWC5 and the third cycle with polyDADMAC and Ag(-) coated SWC5. Three membranes were prepared for each cycle of experiments: with the first membrane a three hour clean water flux test was performed, the second membrane was fouled for three hours with sodium alginate and the third membrane was fouled for two hours with sodium alginate and cleaned for 30 minutes with a pH 3 HCl wash. After all experiments were completed a single experiment of the complete cycle was performed for each set with a single membrane being used for clean water flux, fouling, cleaning and post-cleaning flux recovery.

**Table 6.1.** Experimental matrix for bench scale RO experiments using SWC5 membranes.

<b>Experiment</b>	<b>(+) Coating</b>	<b>(-) Coating</b>	<b>Foulant</b>	<b>Cleaning</b>
1.1	none	none	none	none
1.2	none	none	Na Alginate	none
1.3	none	none	Na Alginate	pH 3 HCl
2.1	pDADMAC	none	none	none
2.2	pDADMAC	none	Na Alginate	none
2.3	pDADMAC	none	Na Alginate	pH 3 HCl
3.1	pDADMAC	Ag(-)	none	none
3.2	pDADMAC	Ag(-)	Na Alginate	none
3.3	pDADMAC	Ag(-)	Na Alginate	pH 3 HCl

## 6.2 RO methods and additional materials

A bench scale reverse osmosis system, diagrammed in Figure 6.1, was used for the RO experiments. An existing LabView program, v38, was used for all experiments. A pump circulated the water through the piping at approximately 800 mL/min and a cooling system maintained the temperature of the recirculating feed water at  $24\pm 2^\circ\text{C}$ . An automated needle valve was used to ramp the pressure to a target of 1000 psi; if the pressure dropped below 985 or above 1005 psi (the two set points used), the valve was automatically adjusted. The clean water permeate forced through the membrane was collected into a beaker on a digital scale recording mass as input for the LabView program to calculate flux. Permeate containers were 1 L in size and emptied after approximately 750-950 mL had accumulated.

An experiment was defined as the tests performed on a single membrane sample (3.1 or 2.2, for example), while the set of experiments for a particular membrane coating was referred to as an experimental cycle. After each experiment in Table 6.1, the membrane coupon was removed and prepared for electrokinetic analysis. A fresh

membrane was used for each experiment. Some repetition occurred between experiments, such as fouling in two experiments of each cycle; the data was used to confirm repeatability of experiments and observe variability between individual membrane coupons.

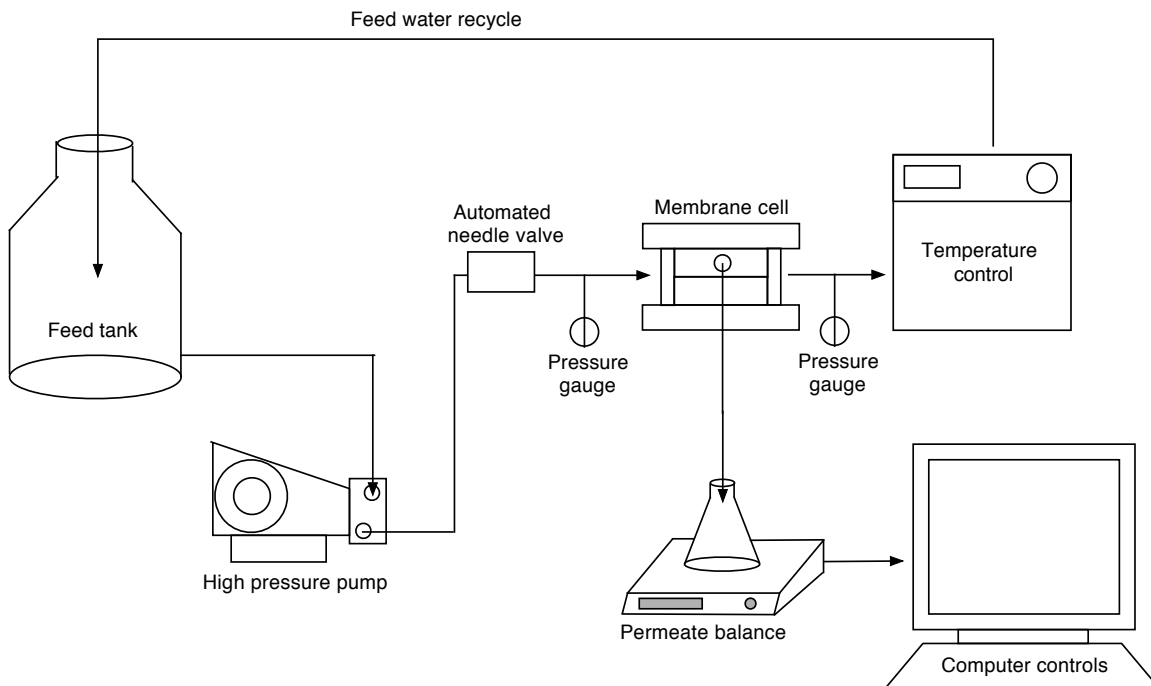


**Figure 6.1.** Diagram of reverse osmosis bench scale filtration system.

A high concentration of sodium alginate was used as a model polysaccharide to foul the membranes and cause flux decline (Mi and Elimelech, 2009; Herzberg et al., 2009). A 2 g/L stock solution was prepared by combining 2 g sodium alginate powder with 1 L of DI water and stirring overnight to dissolve. For fouling experiments, 200 mL of sodium alginate stock solution was diluted into 4 L DI water, resulting in a 95 mg/L sodium alginate solution.

Deionized water flux tests, represented in Table 6.1 by experiments X.1, used approximately 10 L of DI water in continuous recycle mode. DI water experiments ran

for three hours to allow for membrane compaction and evaluate the effects of the different coatings on general flux.

Fouling experiments, represented in Table 6.1 by experiments X.2, started with a one hour clean water flux to compact the membrane. DI water was used in recycle mode for the clean water flux time. After one hour any water remaining in the feed tank was wasted until the water level was just above the pump, at which point the pump was stopped. Sodium alginate feed solution was prepared in a 4 L flask and added to the feed tank. The feed hose was filled with water and the system set back to recycle mode. The program was started and fouling occurred for three hours from the time the system reached the target pressure of 1000 psi. The membrane was removed from the sample holder, the sample cell was bypassed and the system was cleaned with 1 L pH 12 NaOH for five minutes followed by 1 L pH 3 HCl for 10 minutes. At least 20 L DI water was flushed through the system after cleaning.

Membrane cleaning experiments, represented in Table 6.1 by experiments X.3, consisted of one hour DI flux and two hours sodium alginate fouling as described for X.2 experiments. After 2 hr of fouling any remaining solution in the feed tank was wasted until the water level was just above the pump. Four liters of pH 3 (0.001 M) HCl solution was immediately added to the system and recycled through for 30 min. The system was flushed with DI water for at least 5 minutes after acid cleaning to remove residual acid, foulant and coating material from the system, then the membrane was removed and the system cleaned as described for the fouling experiments.

Finally the entire cycle of experiment was performed on a single membrane sample, involving DI water flux, fouling, cleaning and recovery. In the full experiments, membranes were compacted for one hour, fouled for three hours, cleaned with HCl for 30 minutes and DI water was run through the system for at least one hour to evaluate flux recovery after cleaning. The system was flushed with 20 L DI water after full experiments without caustic cleaning.

A six hour DI water experiment was run to evaluate membrane compaction over the course of the experiments. After six hours of DI flux through the membrane a 35 g/L NaCl solution was used to test membrane rejection. Rejection exceeded 99% throughout a one hour experiment. This indicates that despite high flux values (in excess of 120 L/m<sup>2</sup>h), the membranes used for RO experiments had acceptable integrity.

### **6.3 Bench-scale RO results**

The bench scale RO experiments had promising results. Actual flux values are reported in standard units of L/m<sup>2</sup>/hr (lmh) and normalized flux values are reported as a fraction. When fluxes were normalized to the six hour DI water experiment and compared (Table 6.2), the membrane coated with both polyDADMAC and Ag(-) had the best flux recovery after fouling and cleaning. Fluxes for experimental membranes are reported throughout this section in relation to the six hour DI water experiment, which is considered to be 100% flux (maximum flux achievable under experimental conditions) at all times; the flux after four hours, which was reduced from the initial by 10% due to membrane compaction, was considered 100% flux after four hours of experiment time. The six hour experiment accounted for membrane compaction so that experiment cycles

could be compared to a “normal” membrane subjected to the same filtration duration. Results are reported as normalized flux averaged throughout the experiment timeframe (one hour for DI flux, one hour for DI flux after cleaning, etc) except for fouling experiments, in which the last five minutes of flux data is averaged; averaged normalized flux is then compared to that of the SWC5 six hour DI water experiment to determine what degree of flux decline or recovery was achieved after membrane compaction was addressed.

The initial fluxes for all membranes were similar (Figure 6.2), indicating that coatings were not thick enough to cause flux decline. PolyDADMAC-coated SWC5 achieved 98% of uncoated membrane flux while the Ag(-)-coated membrane achieved 97% flux. Some variability was observed between membrane samples ( $\pm 5\%$ , not shown); experiments with similar flux values were compared where possible. Variability was expected due to heterogeneity of the membrane and some user error with the bench-scale unit. Some variability on coated membranes was also attributed to heterogeneity of coatings, which was exacerbated for Ag(-) coatings if the polyDADMAC coating varied significantly.

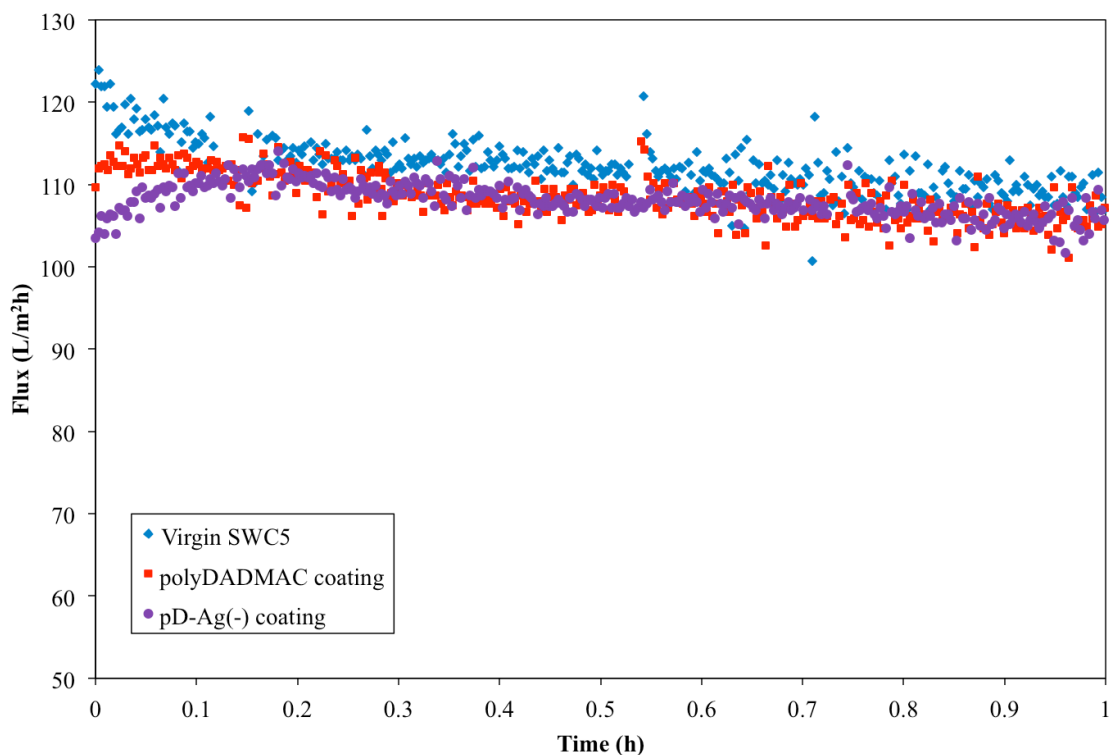


**Figure 6.2.** Comparison of DI water flux. Uncoated SWC5 had the highest flux with polyDADMAC-coated and Ag(-) coated fluxes slightly lower.

In fouling tests (Figure 6.3), the coated membranes fouled at approximately the same rate with an equal overall flux (75% of clean water flux). The uncoated membrane fouled more quickly, resulting in faster flux decline and lower overall flux (66%). There is an offset in Figure 6.3 due to flux being normalized to the six hour DI water experiment rather than the actual flux of each membrane when fouling began. The lower rate of fouling and higher flux for coated membranes indicates that the coatings may block foulants from adsorbing in the “loops and valleys” of the membrane structure. When actual flux values were compared (Figure A.6) it was noted that both coated membranes had lower fluxes when fouling began, but fouled to a lesser extent than the uncoated membrane. The flux for both coated membranes after fouling, which was

indistinguishable in both normalized and actual flux data, was slightly higher (75 lmh) than the uncoated membrane (70 lmh).

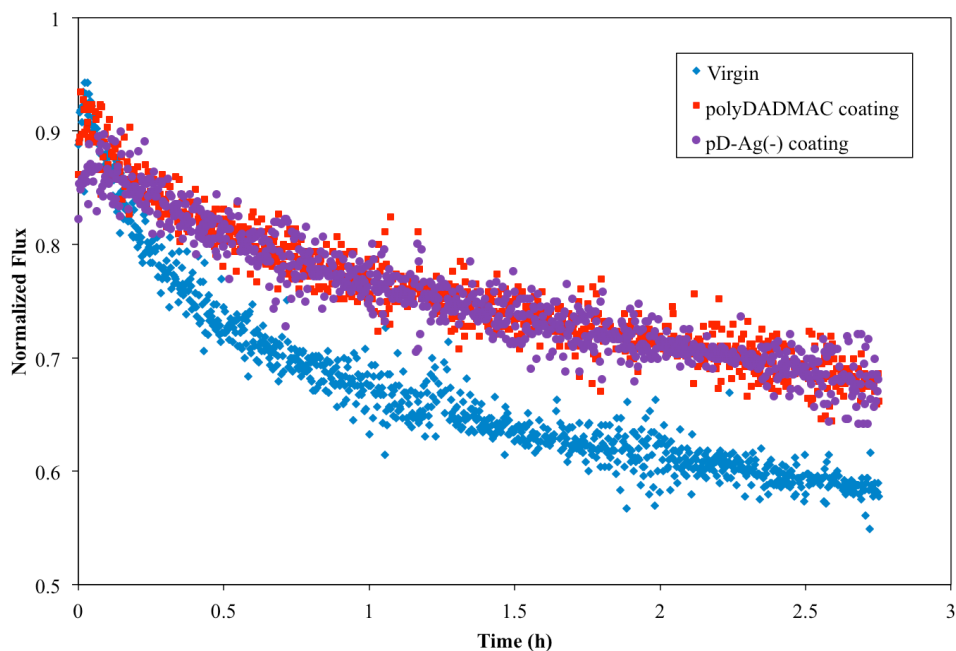


**Figure 6.3.** Fouling of virgin, polyDADMAC coated and Ag(-) coated membranes. Somewhat less fouling occurred on the coated membranes, resulting in 10% higher flux.

Flux recovery experiments after pH 3 cleaning for 30 minutes are shown in Figure 6.4, with polyDADMAC-coated and virgin membranes demonstrating similar recovery. Most notably, Ag(-) coated membranes had improved flux recovery over the virgin and polyDADMAC coated membranes, which suggests that the NP coating improves the removal of the foulant and benefits flux recovery after washing. The flux through each membrane was normalized to the flux of the six hour DI water experiment after four hours of membrane compaction. When actual flux values are compared (Figure A.7), a similar effect is observed. Cleaning of the polyDADMAC-coated membrane shows improvement when normalized flux is considered, but actual flux values are very similar

to the uncoated membrane. When the Ag(-)-coated membrane is cleaned, however, the resulting flux is higher than that of the uncoated membrane.

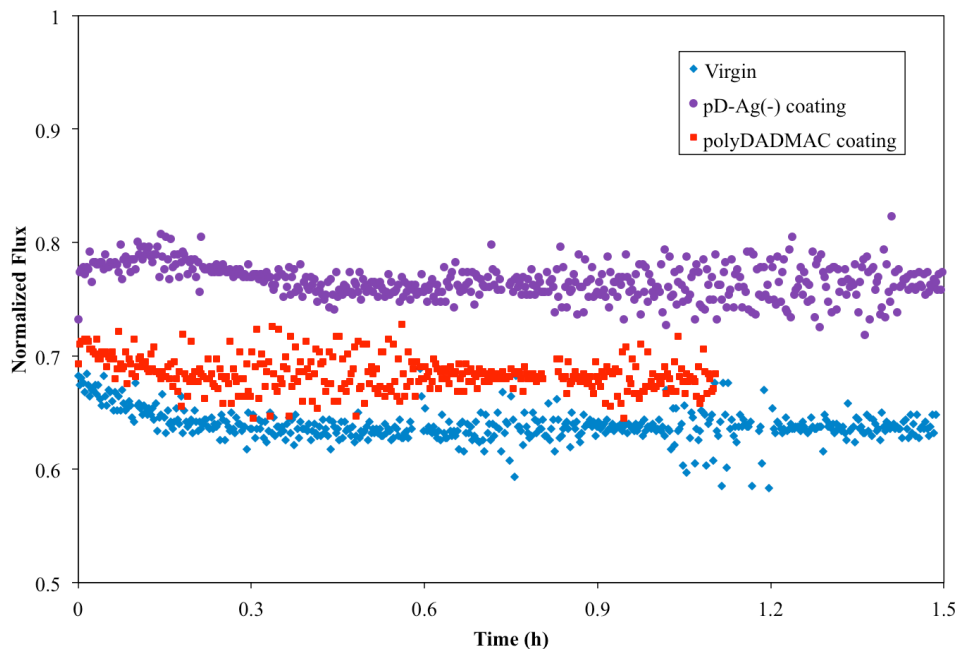


**Figure 6.4.** Flux recovery after acid cleaning. PolyDADMAC coating gives slight improvement in flux recovery, but Ag(-) coating notably increases post-cleaning flux.

Repeated parts of experiments (fouling occurred on two of the three membranes in each experimental cycle, for example) were compared to determine the repeatability of RO flux test results. Flux data in these figures are normalized to the first flux measurement of each experiment for comparison purposes. DI water flux data were compared from three separate Ag(-) coating experiments (Figure 6.5). Data were comparable except for an anomalous initial flux on 5/23/2012. DI flux data for polyDADMAC-coated membranes were similar. SWC5 fouling experiments are more varied than DI water experiments (Figure 6.6). Experiments differ in rate of fouling and final flux after fouling.

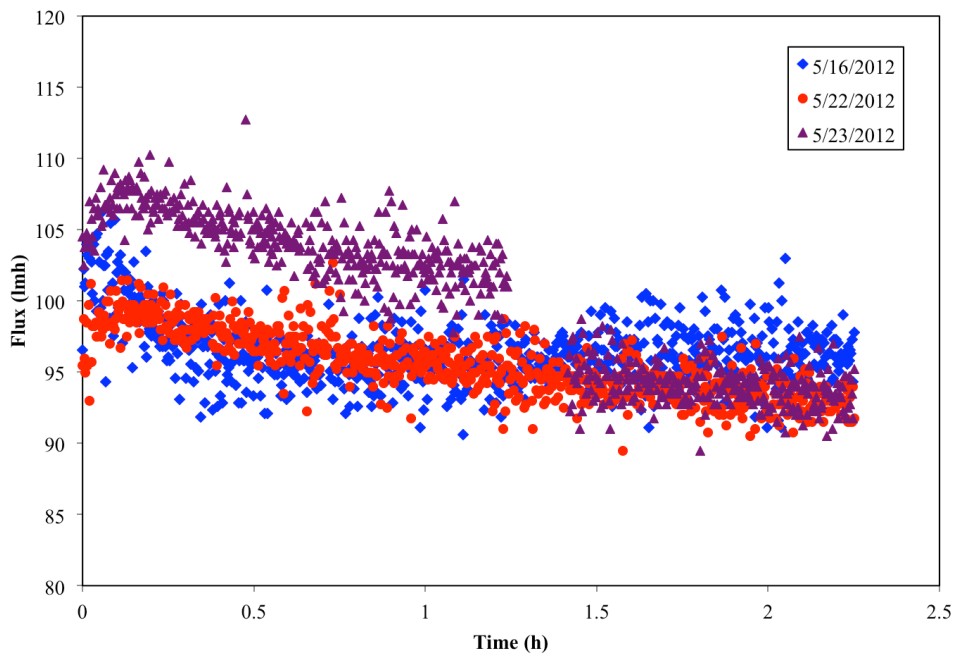


**Figure 6.5.** Comparison of DI water flux for Ag(-) coated SWC5 membranes. The third data set suddenly dropped by approximately 5% flux after 1.5hr, which cannot be explained with the data available.

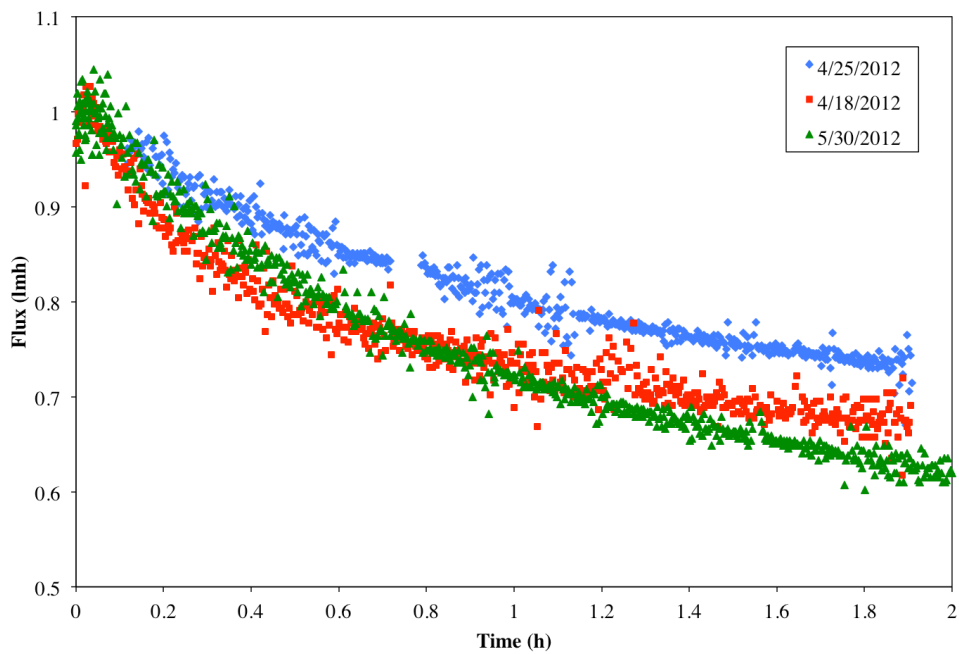


**Figure 6.6.** Comparison of SWC5 fouling experiments. Fouling experiments were more varied than DI water flux. Different rates of fouling and flux declines are observed.

The complete cycle of experiments consisted of DI water flux for 1.3 hours, sodium alginate fouling until 4.1 hours, pH 3 HCl cleaning for 30 minutes and DI water flux recovery after cleaning. Cleaning was performed at low pressure and flux data were not collected, so flux recovery data were modified by approximately 30 minutes for continuity of Figure 6.7.

In the full cycle experiment, a clean water flux was run through a SWC5 membrane for six hours to evaluate membrane compaction effects. Improved flux recovery was expected for the coated membranes when compared to the uncoated membrane. Both coated membranes had slightly higher DI water flux than the uncoated SWC5. Fouling occurred more slowly on coated membranes than for SWC5, with 10% higher flux through coated membranes. Flux recovery for the Ag(-) coated membrane showed notable improvement over both polyDADMAC-coated and uncoated SWC5, achieving 83% flux after pH 3 HCl cleaning compared to 74 and 69% of DI water flux, respectively. With respect to Figure 6.7, the average flux of the SWC5 DI flux is considered to be 100% throughout the experiment such that the 83% flux of the Ag(-) coated membrane is relative to the SWC5 membrane after four hours of membrane compaction.

**Table 6.2.** Average flux normalized to SWC5 DI water experiment after each stage of RO filtration.

Membrane	Initial Flux (lmh)	Averaged Normalized Flux			
		DI water	Fouling	Post-cleaning	Final
SWC5	122	0.907	0.664	0.639	0.690
SWC5-pD	113	0.958	0.751	0.684	0.739
SWC5-pD-Ag	112	0.954	0.751	0.766	0.827

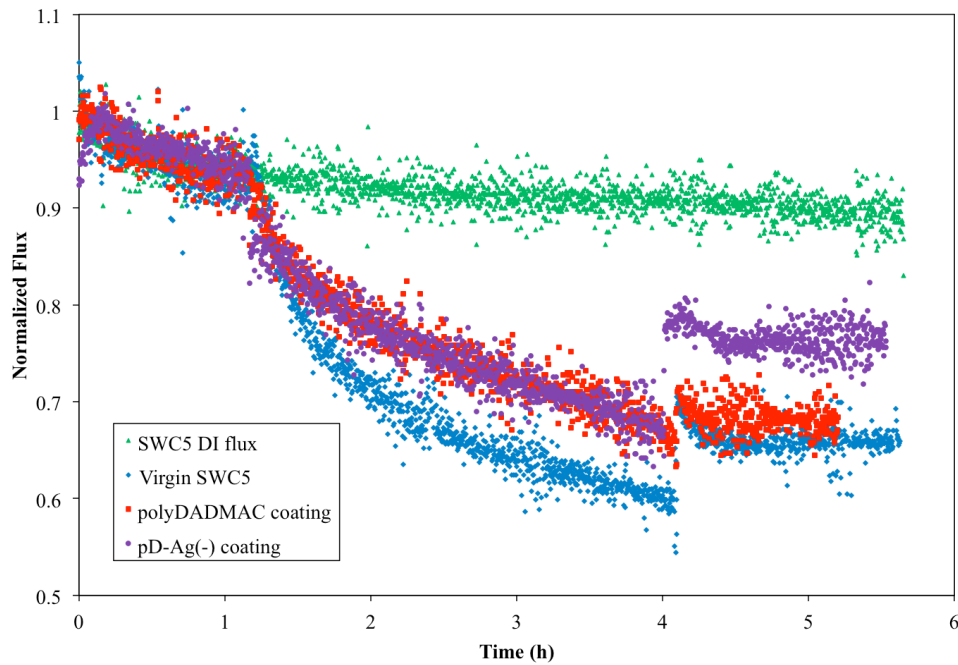


**Figure 6.7.** Full cycle RO experiments. PolyDADMAC and Ag(-) coatings had lower initial flux and slower fouling. Ag(-) had notable flux improvement after cleaning.

Overall, the coating concept showed promise in the RO experiments. PolyDADMAC and Ag(-) coated membranes did not significantly decrease the flux of the membrane. Fouling occurred to a lesser extent, with less flux decline, on coated membranes. Nanoparticle coated membranes showed notable flux improvement after simple acid cleaning. Future experiments need to be performed in saltwater conditions so salt rejection, the most important aspect of desalination membranes, can be considered. Coatings should be re-applied in the RO system to determine feasibility of the regenerable coating concept.

## CHAPTER SEVEN

### CONCLUSIONS AND RECOMMENDATIONS

Considerable progress has been made toward the goal of determining whether the materials used in this study can be electrostatically applied and removed. Coatings demonstrated success in delaying fouling of the membranes and cleaning experiments in the bench-scale RO system indicated that coating removal may improve flux recovery after fouling. This chapter aims to summarize the progress toward the main research goal and suggest future experiments and analyses.

#### **7.1 Conclusions relating to research objectives**

*7.1.1 Determine appropriate conditions for self-assembly of polymer and NP coatings on RO membranes.*

The polymer and NPs selected for this study were novel materials for RO membrane coatings. PolyDADMAC is currently used in the water treatment industry as a flocculant and would be simple to implement in RO systems if effective. PolyDADMAC had also been previously demonstrated to cause few negative changes to the membrane when explored in an operational context (Gabelich et al., 2005). NDMA formation is not a concern in drinking water treatment operations because oxidative disinfectants are not used; they are detrimental to polyamide membranes. However, polyDADMAC has been demonstrated to decrease antiscaling membrane properties when used as a coagulant in pretreatment trains prior to RO filtration (Kim et al., 2009). Diluted solutions of polyDADMAC (0.2% w/v) effectively coated the polyamide membranes, causing a large

increase in zeta potential throughout the pH range investigated (3 – 9) and negligible flux decline under normal operating conditions in DI water.

Functionalized inorganic-polymer composite NPs are a model system useful for the fundamental work performed here, though their applicability in full-scale systems may be cost-prohibitive. Future work with this project may continue to use the NPs purchased for this study, but consideration should be given to whether NP use is economically or ecologically feasible. There are environmental concerns regarding behavior of nanomaterials in natural systems (Auffan et al., 2009); on the large scale, a process would need to be implemented to remove and dispose of NPs after removal. The effects of the inorganic component, such as any antifouling properties, should also be considered; no significant difference was observed between  $\text{TiO}_2(-)$  and  $\text{Ag}(-)$  when measurement variability was considered, suggesting that the functionalizing polymer (polyacrylate) dominated mechanisms of adsorption to the membrane. Small quantities of NPs – 3.8 mg Ti/L  $\text{TiO}_2(+)$ , 4.2 mg Ti/L  $\text{TiO}_2(-)$  and 20 mg Ag/L  $\text{Ag}(-)$  NPs – were able to cause notable zeta potential changes on the membrane surface. The percent coverage of the membrane and coating heterogeneity have not yet been determined.

Coating methods were developed over the course of this study. When experiments began, dry membrane coupons were placed directly into coating solution and coated statically at low temperature (4°C). As experiments progressed and implementation was considered, coating conditions were modified to more closely emulate the operating conditions of an RO facility. In an RO plant, coating and cleaning membrane modules would be accomplished by passing the solution over the membrane surface at ambient

temperature (~25°C). Membrane modules are inspected by the manufacturer and vacuum-sealed in water before purchase, so all membranes being coated would already be saturated with water. From August 2011 onward, membrane coupons were soaked at least overnight before being immersed in the coating solution. A rocker table was used to agitate the coating solution to move continuously across the membrane surface, creating dynamic coating conditions expected in a RO plant.

#### *7.1.2 Determine appropriate conditions for coating removal.*

All coatings were at least partially removed by acid cleaning, as indicated by zeta potential measurements and SEM imaging. Zeta potential titrations indicated that polyDADMAC remained on the membrane surface after cleaning with all acid concentrations, likely due to the polymer adsorbing at multiple sites on the membrane or getting “stuck” in the loop and valley structure of the membrane surface. Alternative binding mechanisms, such as van der Waals interactions, may also have played a role in polyDADMAC adsorption after acid cleaning. If binding was truly electrostatic, polyDADMAC should have been repelled from the membrane surface as high proton concentrations “crowded out” the negative charge density on the membrane surface (Figure 7.1a).

Negatively charged Ag and Ti NPs were removed by acid cleaning because they were bound to the polyDADMAC layer; when the polyDADMAC was repelled from the membrane, the NPs were removed as well. The few base cleaning experiments performed indicated some removal of the negative NPs but endurance of the polyDADMAC coating. This was an expected result for electrostatic interactions (Figure 7.1b). SEM

imaging of Ag(-) aggregates indicated that NPs remained on the surface after strong acid cleaning but were removed by strong base cleaning. Base cleaning was not pursued because it was not as effective in removing the polyDADMAC as acid cleaning; experiments were focused on removal of all coatings, so NPs were removed via removal of polyDADMAC.

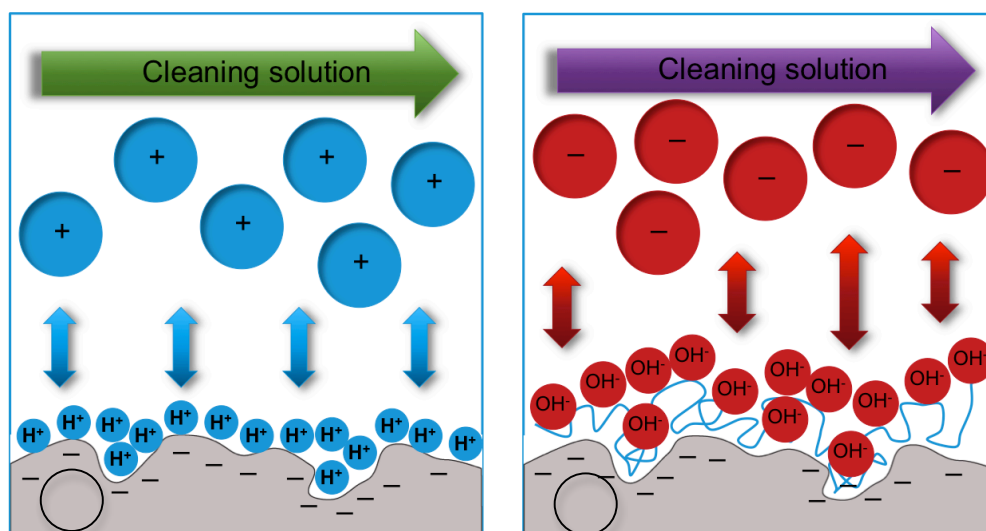


**Figure 7.1.** Expected desorption mechanisms for positive materials at low pH (a) and negative particles at high pH (b). PolyDADMAC and TiO<sub>2</sub>(+) were expected to detach from the membrane via mechanism (a) while negatively charged NPs were expected to detach from the polyDADMAC layer via mechanism (b).

There remains a question of whether NPs can be removed from the membrane if they are entrapped in the loop and valley structure. PolyDADMAC coating was observed “filling in” the loop and valley structure in several SEM images (Figure 4.12; Figure C.5), which could prevent NPs from becoming trapped. Additionally, the only goal of removing the coating materials is to remove foulants; if some NPs remain on the membrane after cleaning but foulants are removed, the end goal has been accomplished. Coatings that adsorb within the loop and valley structure also occupy active sites where undesirable materials may adsorb or accumulate, such as bacteria and mineral deposits.

### *7.1.3 Use zeta potential titrations to detect the presence of self-assembled coatings.*

Zeta potential measurements were used throughout the study to detect the presence of membrane coatings. Zeta potential measurement was the only way to detect the coatings in most cases; though polyDADMAC coating was not visible to ATR-FTIR or low to moderate magnification SEM, the adsorbed material caused significant changes to the zeta potential of the membrane, confirming its presence. The same was true for both TiO<sub>2</sub> NPs, and lower concentrations of Ag(-) NPs, which were not visible on SEM. Comparison of zeta potential single measurements with SEM images of coated and cleaned Ag(-) NP aggregates allowed more complex conclusions to be considered.

## **7.2 Future work recommendations**

### *7.2.1 Materials and material characterization*

Quantification of the polyDADMAC polymer was not performed because a suitable method was not determined during the course of this study. Total organic carbon or total nitrogen analysis of the coating solution and reverse osmosis permeate may be effective methods for detecting polyDADMAC in solution; comparison to the 20% stock solution provided by the manufacturer should allow for quantification of the samples.

Several methods were available for quantification of NPs but only one was used. Quantification of Ti NPs is particularly important because solutions were prepared from powdered NPs that were observed sticking to glassware after preparation. The inorganic component of each NP was targeted during analysis; in this study, ICP-OES determined the concentration of Ag or Ti present in stock solution samples acidified with 5% HNO<sub>3</sub>. Low Ti NP concentrations indicated that NPs were incompletely dissolved in simple acid

solution and digestion should be performed for further analysis. Digestion was not undertaken for the solutions discussed in this study but there is confidence in the measurements of Ag(-) NPs, which was as expected. A microwave digestion instrument is available for use and acid digestion SOPs were obtained; comparison between the two digestion methods would be interesting. ICP analysis of Ag(-) NPs produced the expected result, so further analysis is probably only necessary to produce a calibration curve at higher concentrations.

Zeta potential titrations at different stages of the study revealed significant variation in NP coatings that were applied using the same process. It is suspected that Ti NPs may have aggregated in the stock solutions after being stored for several months, resulting in a large variation in concentration between aliquots of NP solution. While size analysis was reported by the manufacturer for the Ag(-) solution and powdered TiO<sub>2</sub> NPs, verification of NP size in stock solutions would be beneficial. Differences between values reported by the manufacturer and laboratory measurements may indicate whether aggregation occurred when dissolving NPs in DDI water. Future stock solutions may be prevented from aggregating by sonicating solutions occasionally during storage and before aliquots are removed for membrane coating.

The NPs adsorbed to the membrane surface should be quantified. Acid digestion of the membrane coupons can be used to release the Ti and Ag from the functionalizing polymer and the membrane surface; these concentrations can be used to infer the quantity of inorganic components on the membrane. Because both sides of the membrane are exposed to NPs during coating, it must be taken into account that Ti or Ag values from

ICP analysis will include NPs bound to the backing layer as well as the active layer. This method does not address how many inorganic components are present in each NP or how NPs are distributed on the membrane surface, nor percent coverage.

### *7.2.2 Coating condition optimization*

Coating kinetics were briefly examined to determine NP coating duration, but kinetics did not fit the scope of this study. Kinetics should be investigated more thoroughly, similarly to the concentration experiments in this work, seeking the shortest effective coating time. It is expected that coatings assemble electrostatically on the order of minutes. Reducing the duration of coating time may reduce the cost of implementing this technology.

Verification of coating layers by a technique other than zeta potential would be useful; X-ray spectroscopy is expected to be a viable option. X-ray photoelectron spectroscopy (XPS) is used for elemental characterization of membrane surfaces and can be employed to verify the presence of Ti and Ag on the membrane (Siegbahn, 1981). XPS requires concentrations of parts per thousand or higher, which may present issues with the extremely thin NP coatings. Parts per million concentrations are detectable, but longer data collection times or specialized instrumentation are required. Energy-dispersive X-ray spectroscopy (EDS), a technique coupled to SEM instrumentation, can also be used for elemental analysis of the sample. Sputter-coating may interfere with detection of small quantities of Ti or Ag, so samples that are not sputter-coated should be analyzed. Samples may then be sputter-coated for SEM visual analysis.

Both X-ray techniques are critical tools, as the top 1-10 nm of the material can be analyzed; compared to ATR-FTIR, which produced a spectrum dominated by the polysulfone membrane backing, these techniques are highly sensitive (Tang et al., 2009a). No interference is expected for either Ag or Ti detection due to the organic nature of the membrane structure, functionalizing polymers and polyDADMAC coating. Trace amounts of other elements in the NPs, analyzed and reported by the manufacturer in the technical specification sheet, would produce negligible if any response.

SW30HR, the membrane used for most of the experiments, had a commercially applied PVA layer that prevented significantly high (+30 mV) or low (-30 mV) zeta potential from developing at the membrane surface. Though this property is beneficial in operating conditions, the shielding of the PA surface layer decreased the electrostatic strength of membrane interactions and may have prevented coatings from being fully adsorbed or removed. Electrostatically unfavorable conditions would likely develop on SWC4 and SWC5 membranes; effects might not be observable on SWC5 in the pH range of titrations since the isoelectric pH is  $\sim 3$ , but comparable experiments using SWC4 could confirm conclusions drawn from SW30HR experiments.

### *7.2.3 Removal of coatings*

Base solutions of various strengths should be investigated in the future to determine whether foulants could be removed by cleaning of the NP coating alone; however, from an application perspective, polyDADMAC is inexpensive enough to justify pursuing acid cleaning alone.

#### *7.2.4 Bench-scale RO fouling experiments*

Reverse osmosis experiments were promising, with the nanoparticle-coated membrane having the highest relative flux recovery as well as less flux decline than the uncoated membrane during fouling. Despite some flux improvement, sodium alginate was visible on all fouled membrane samples removed from the bench scale unit. The fouling layer may have been too thick for the acid cleaning solution to effectively repel the polyDADMAC coating from the membrane surface; the quantity of foulant used represented a worst-case scenario for fouling.

Additional RO fouling experiments should be performed in saltwater solutions so salt rejection data can be collected and the comprehensive effects of membrane coatings can be evaluated. Different types of foulants should be tested as well to determine whether the coating materials are effective against multiple modes of fouling. To evaluate whether coatings are “regenerable” and could be reapplied, application of coatings in the bench scale system should be attempted.

Future studies of this research topic should focus on bench-scale experiments. Though membrane characterization is useful and method development necessary, coatings must be applicable in a system to be of any benefit. In RO experiments, salt water should be used to determine feed water chemistry effects on coatings. Coatings can be explored with other types of membranes as well to be applied to other systems, though adsorption within pores will need to be considered in the case of MF and UF membranes (Luxbacher, 2006).

## APPENDICES

Appendix A

Additional Images

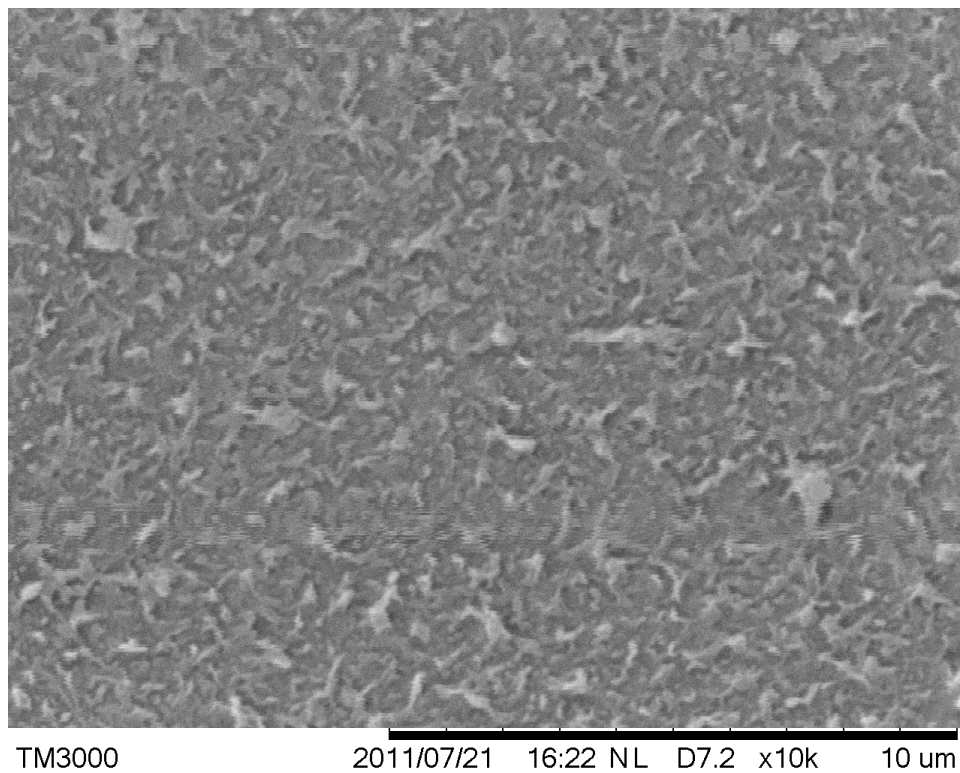


**Figure A.1.** SEM image of SW30HR membrane coated with 0.2% polyDADMAC and 3.7 mg/L TiO<sub>2</sub>(-).

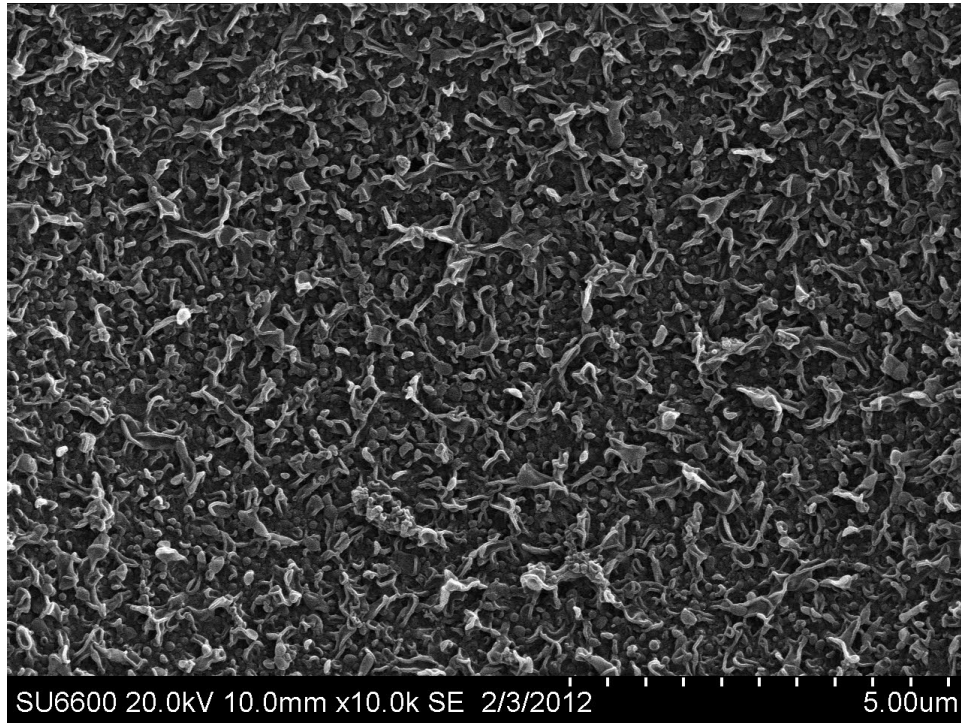


**Figure A.2.** SEM image of SW30HR membrane coated with 0.2% polyDADMAC and 20 mg/L Ag(-).

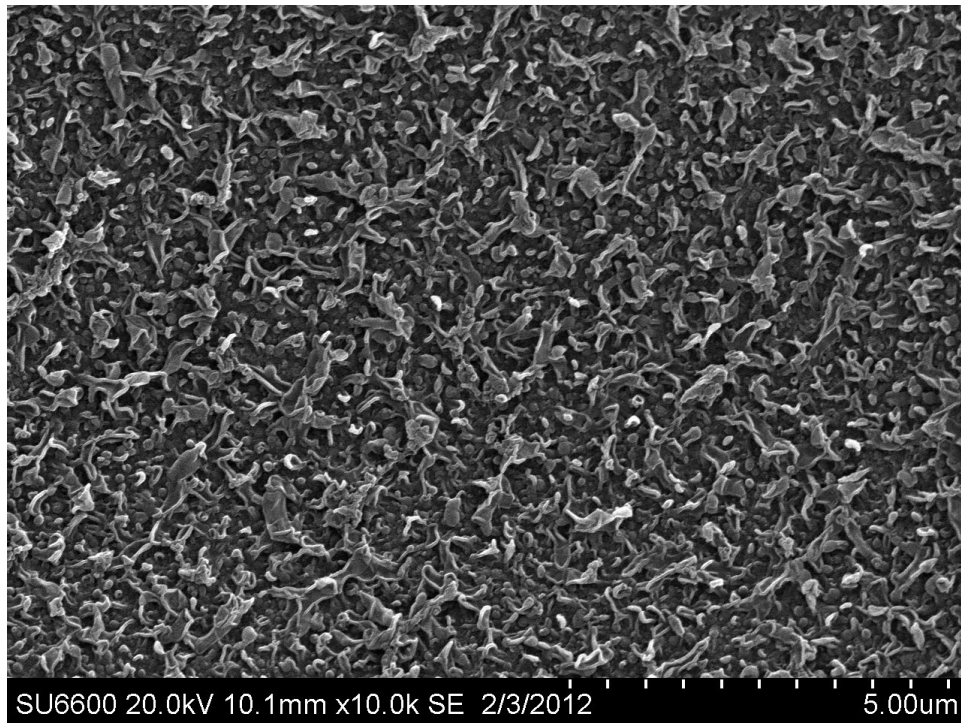


**Figure A.3.** SEM image of uncoated SW30HR membrane.

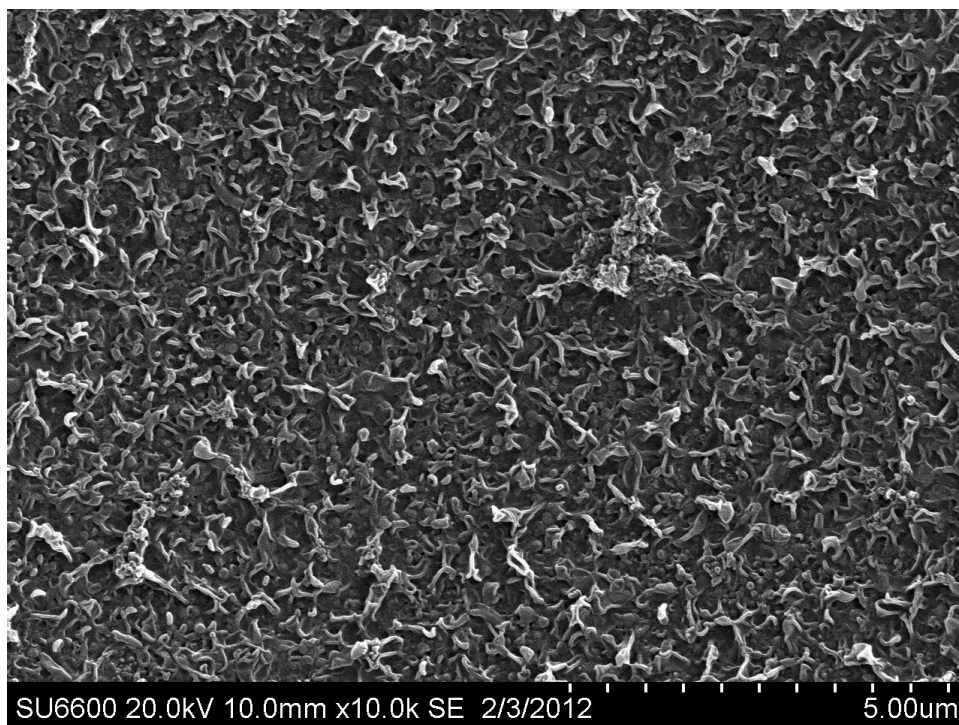


**Figure A.4.** SEM image of SW30HR coated with 0.2% polyDADMAC. The clump of material in the upper right quadrant of the image is an artifact of membrane formation.

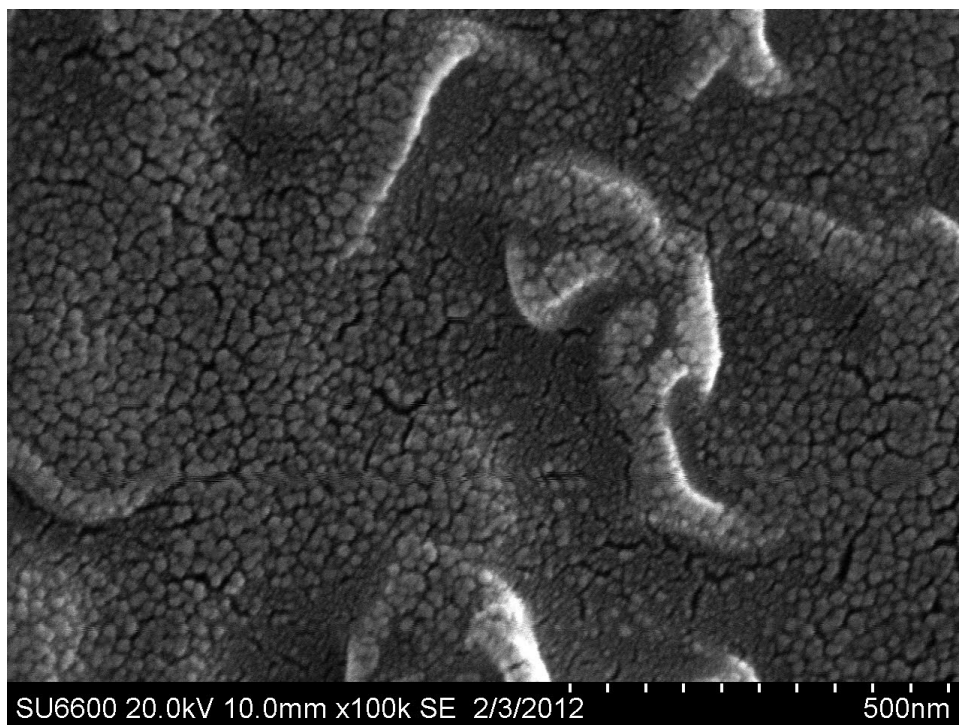


**Figure A.5.** SEM image of SW30HR coated with 0.2% polyDADMAC. This section of the membrane shows the “filled in” loop and valley structure.

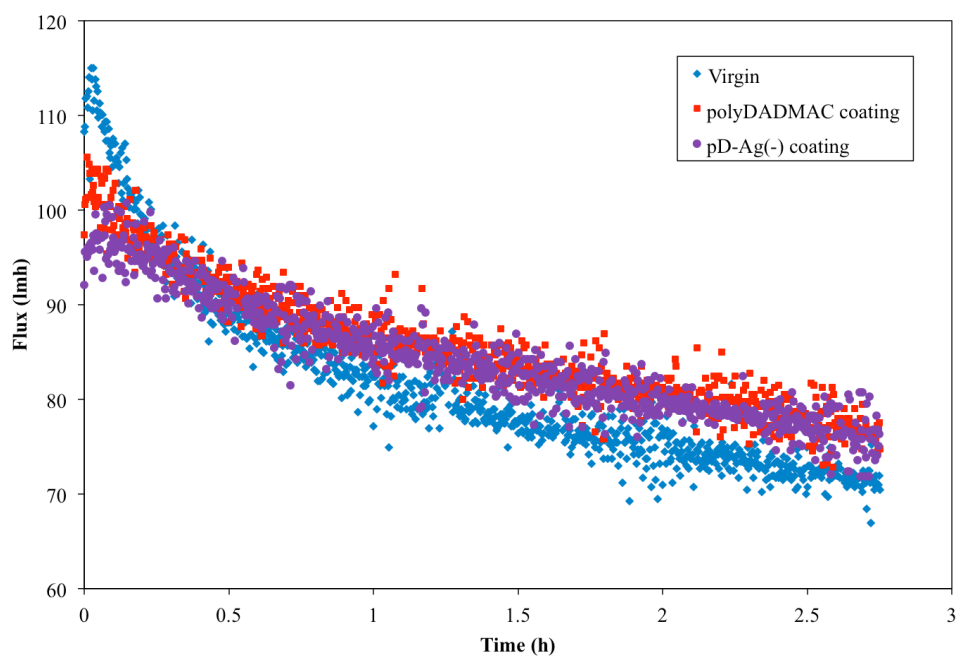


**Figure A.6.** Actual flux values for uncoated, polyDADMAC-coated and Ag(-)-coated SWC5 membranes. While the fluxes of the coated membranes were lower when fouling began, fouling occurred less dramatically overall for both coated membranes.

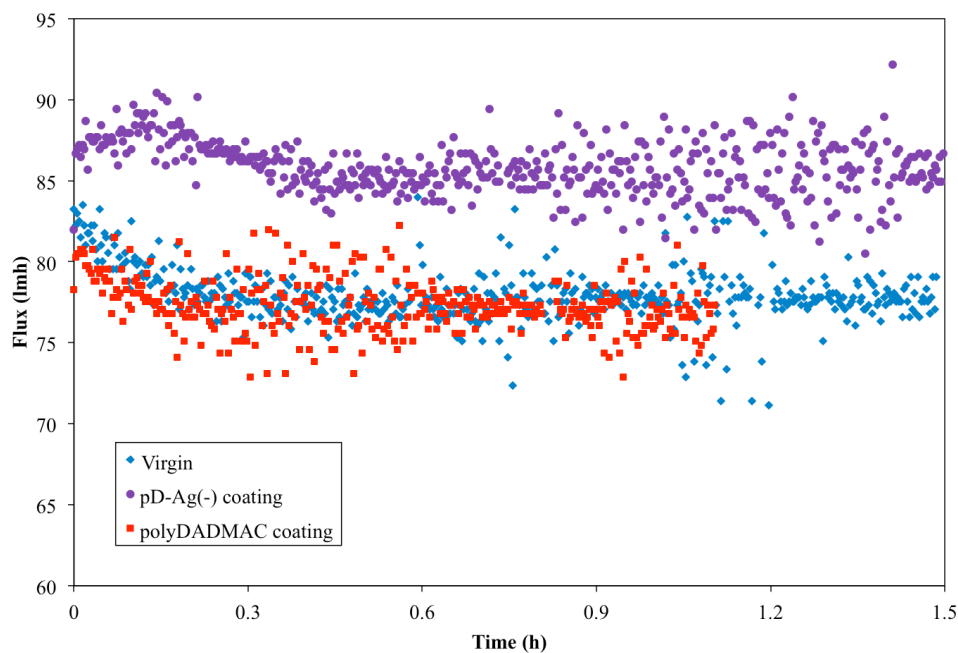


**Figure A.7.** Actual flux values for uncoated, polyDADMAC-coated and Ag(-)-coated SWC5 membranes after acid cleaning. Cleaning of the Ag(-) membrane resulted in a notable improvement.

## Appendix B

### SurPASS Adjustable Gap Cell: Standard Operating Procedures

#### ***Night-before Preparation***

1. Cut membrane coupons (~1"x0.5") and soak in DDI water overnight.
2. Prepare 1 mM KCl solution:
  - Pipet 10 mL 0.1 M KCl solution into 1000 mL volumetric flask.
  - Fill to mark with DDI water.
  - Vacuum filter KCl solution:
    - Rinse Whatman funnel with DI water.
    - Position a 1  $\mu$ m, 47mm membrane and assemble unit.
    - Rinse membrane by filtering 50-100mL DDI water; discard.
    - Filter KCl solution.
    - Clean up: rinse used glassware 3x with DI water and place on drying rack.

#### ***Adjustable Gap Cell Assembly***

1. Adhere double-sided tape to blue sample holder. Press out bubbles.
2. Peel backing off tape and adhere backing of membrane to tape.
  - Pull overhanging edges firmly with tweezers; press with Parafilm if needed.
3. Trim membrane to exact size of sample holder.
  - Exercise extreme caution to not damage the sample holder with scissors.
4. Insert sample holders into AGC.
5. Adjust gap so both sides appear equal – a very thin slit of light should be visible from each side.
6. Allow knurled nuts to freely spin onto sample holder stems until they stop at the AGC. Place holders and fold down arms to secure.
7. Tighten knob on top of AGC until finger tight.
8. Double check gap on both sides to ensure gaps are equal.
  - ▲ If gaps are not equal, disassemble to step 5 and readjust before proceeding.
9. Insert the leads into the perfusion holes.
10. Adjust the AGC holder to align with the grooves in the leads. Press down gently. Adjust if needed.
11. Attach the AGC and tighten the leads with the knob on the holder until the clutch engages.

#### ***Instrument Startup***

1. Start up VisioLab for SurPASS.
2. Turn instrument on.
3. Fill 600 mL Schott beaker with 500 mL 1 mM KCl. Add stir bar.
4. Open *Pre-Measurement* window and run *Fill* cycle for 100 s.
5. Run *Rinse* cycle to determine gap height:

- Start *Rinse* cycle.
  - When first ramp achieves target pressure (-300mbar), observe gap height readings.
  - If instrument fails to achieve target pressure, narrow gap height and repeat *Rinse*.
  - Adjust gap height as necessary to reach  $0.105 \pm 0.01$  mm.
6. Run full *Rinse* cycle for 300s after acceptable gap height is achieved.
  7. Run *Flow check* at 300mbar. Record final pressure and flow for each ramp.
    - If either ramp is nonlinear or does not achieve target pressure ( $\pm 50$  mbar), re-run *Flow check*.
      - It may be necessary to take apart the AGC and check the membrane, reverse the orientation of the AGC, re-run and closely observe the *Rinse* cycle, or undertake other troubleshooting measures.
  8. If running titrations and machine has been **OFF**, switch to beaker of 500 mL DI water and rinse syringes to clear bubbles from tubing:
    - Open *Setup* window and select *Titration Settings*.
    - Rinse both Left & Right syringes for 2 rinse cycles **into DDI water, not the KCl solution**.

### **Membrane Analysis**

1. Run HCl titration:
  - File → New Measurement Document from Template (Ctrl+T)
  - Select “Adjustable Gap Cell.stf”
  - Fill appropriate sample description: material, pore size, coating, etc.
  - Select appropriate user (YOU!).
  - Measurement Type → pH Titration
  - Under *pH Titration*, change *Used Syringe* to *Syringe Right (HCl)*.
  - Return to *Sample Settings* and **START** titration.
  - Save file: “year-month-day (sample description) HCl”
    - .1. E.g., **2011-01-01 SWC4 virgin membrane HCl.srf**
2. *Rinse* instrument 3x with DDI water – pH reading should return to ~5.5.
3. *Rinse* instrument 1x with fresh KCl solution.
4. Run NaOH titration using same procedure as HCl, except:
  - Do NOT change *Use Syringe* settings.
  - Change *pH Maximum* to 9.
  - Change *Desired pH difference* to 0.25
  - Save file: “year-month-day (sample description) NaOH”
    - .1. E.g., **2011-01-01 SWC4 virgin membrane NaOH.srf**
5. *Rinse* instrument with DDI water at least 3x until pH stabilizes between ~5.5.

### **Instrument shut-down**

1. After pH has stabilized:
  - If instrument has been run for 2+ titrations, set *max. Time for Empty* cycle to

500s.

- If instrument has been run for a single titration, set *max. Time* to 300s.
  - Fill 600mL Schott beaker with DDI water.
  - Disconnect the outlet hose from beaker cover and put it in the DDI beaker.
  - Place the beaker cover with inlet hose onto an empty beaker.
  - Start the *Empty* process in the *Monitor* window of VisioLab.
2. If instrument is suspected to be contaminated by desorbed coatings, see SurPASS instruction manual for appropriate cleaning measures (pg 60).
  3. Turn instrument off.
  4. Disassemble AGC.
  5. Discard used membranes.

## Appendix C

### Bench Scale RO for Membrane Coatings: Standard Operating Procedures

#### ***Night-before Preparation***

- Add 200 mL of sodium alginate to 4 liters of DI to make fouling solution.
- If cold, bring water sample to room temperature overnight.
- If membrane is not already in DI water, cut coupon and place in DI water.
  - Membranes for coated experiments should be pre-coated and soaked in DI water at least overnight.

#### ***Clean-water flux run***

- DI should be in the system after the cleaning.
- Calibrate conductivity meters. (50 mS for on-line meter, 0.447 mS for bench-top meter)
- Set up the system by bypassing the membrane cell and using small plastic Nalgene feed reservoir.
- Calibrate computer clock.
- Tare pressure gauge. Don't tare flow meter; I think it drifts less than taring makes it change.
- Start "RO Control 38.vi"
  - Set Actuator valve voltage to 10V
  - Run software
  - Set pump control to Manual, 4 Hz
  - Turn ON pump inverter to start pump
  - Increase pump speed to 7 Hz
  - Make sure there is no air in the pump intake hose
- Run DI at high pressure. If pulsating, let it run at low pressure for several minutes, or run at about 300 psi, 7 Hz, until pulsation dampens. (Be sure that bubbles have left the DI before running.)
  - Click Actuator valve auto control to ON
  - Set upper limit to 5 psi, lower limit to 15 psi
  - Run at high pressure until system stabilizes; check for leaks at joints
- Run membrane baseline flux/rejection before each fouling experiment. This will require attaching SEPA cell, establishing flux/rejection, wasting DI water and then adding foulant solution.
- Run the DI out until water level is just above pump (don't let air get into the pump).
- Add the fouling solution of 200 mL of 2 g/L sodium alginate in 4 liters DI water.
- Run system to mix foulant with water already present.
- Set up membrane cell:
  - Place membrane coupon in cell WITHOUT spacer
  - Active side toward O-rings
  - Use permeate carrier from Hydranautics brackish water module
  - Pressurize cell to 1200 psi using hydraulic pump
  - Hook up to the system

- Membrane type \_\_\_\_\_ and coatings \_\_\_\_\_
- To start computer data collection:
  - Run system at 7 Hz pump speed (6.4 Hz on controller)
  - Set actuator valve to completely open (10 Hz)
  - Start computer data collection (arrow button on top toolbar at left)
- Write down file name and start time \_\_\_\_\_
- Turn ON actuator valve auto control. Make sure upper limit is set to 5 psi and lower limit to 15 psi.
- Run at constant 1000-psi pressure and manually input Temperature reading at least every 30 minutes. If temperature has not changed, input different temperature and then return to actual temperature 1 minute later. When you are reading data, this confirms that temperature was monitored although not changing.
  - Check and record gauge pressure (just prior to Sepa cell): \_\_\_\_\_
- Turn off program:
  - Set actuator valve to completely open (10 Hz)
  - Set pump to zero in Labview
  - Turn OFF pump inverter to stop pump
  - Use the STOP button on Labview screen to stop data recording.

***Cleaning (must be done after fouling)***

- The system should be sitting in DI from the previous run.
- Run the DI out until water level is just above pump.

After fouling:

- Fill small feed tank with 1 liter of pH 12 sodium hydroxide solution (0.4 g into 1 L)
- Run through for 10 minutes in recycle mode to remove foulants, then drain to just above the level of the pump.
- Run through at least 20 L of DI water without recycle.
- Make sure conductivity of the exit stream ends at close to conductivity of DI water:
  - Example: input of 25 mS DI water and output of 29 mS.

General maintenance:

- Fill small feed tank with 1 liter of 10% phosphoric acid (H<sub>3</sub>PO<sub>4</sub>) solution (117 ml of 85% H<sub>3</sub>PO<sub>4</sub> added to DI water to make 1 liter).
- Run through for 20 minutes (10 minutes for H<sub>3</sub>PO<sub>4</sub>) in recycle mode to remove rust and particulates. (Note that after adding to DI, the acid concentration is lower than 10% and that is fine). Do not leave running much more than 20 minutes (15 minutes for H<sub>3</sub>PO<sub>4</sub>).
- Run through at least 28-l of DI water, without recycle.
- Make sure conductivity of the exit stream ends at close to conductivity of DI water

- Example: input of 25 mS DI water and output of 29-mS.
- Example: input of <5 mS DI and output of 8 - 9 mS.
- Leave system full of DI water.

***Shutdown***

- Turn off program, then shut down system.
- Remove membrane from cell. Cut membrane samples for electrokinetic analysis and refrigerate in DDI water.
- If it's late and you won't be doing cleaning today, run 20 L DI water through the system.
- Leave system in DI water over night.
- Rinse conductivity probe with DI water. Leave to dry.

## REFERENCES

- Al-Amoudi, A.; Williams, P.; Mandale, S.; Lovitt, R.W. Cleaning results of new and fouled nanofiltration membrane characterized by zeta potential and permeability. *Sep Purif Technol* **2007**, 54, 234-240.
- Auffan, M.; Rose, J.; Bottero, J.Y.; Lowry, G.V.; Jolivet, J.P.; Wiesner, M.P. Towards a definition of inorganic nanoparticles from an environmental, health and safety perspective. *Nature Nanotechnol* **2009**, 4 (10), 634-641.
- Ba, C.; Ladner, D.A.; Economy, J. Using polyelectrolyte coatings to improve fouling resistance of a positively charged nanofiltration membrane. *J Membr Sci* **2010**, 347 (1-2) 250-259.
- Bae, T.; Kim, I.; Tak, T. Preparation and characterization of fouling-resistant TiO<sub>2</sub> self-assembled nanocomposite membranes. *J Membr Sci* **2006**, 275 (1-2) 1-5.
- Belfer, S.; Purinson, Y.; Kedem, O. Surface modification of commercial polyamide reverse osmosis membranes by radical grafting: An ATR-FTIR study. *Acta Polym* **1998**, 49, 574-582.
- Braghetta, A.; DiGiano, F.A.; Ball, W.P. NOM accumulation at NF membrane surface: Impact of chemistry and shear. *J Environ Eng* **1998**, 124 (11) 1087-97.
- Brant, J.A.; Childress, A.E. Assessing short-range membrane-colloid interactions using surface energetics. *J Membr Sci* **2002**, 203, 257-273.
- Brant, J.A.; Childress, A.E. Colloidal adhesion to hydrophilic membrane surfaces. *J Membr Sci* **2004**, 241 (2) 235-248.
- Buksek, H.; Luxbacher, T.; Petrinic, I. Zeta potential determination of polymeric materials using two differently designed measuring cells of an electrokinetic analyzer. *Acta Chim Slov* **2010**, 57, 700-706.
- Cahill, D.G.; Freger, V.; Kwak, S.Y. Microscopy and microanalysis of reverse osmosis and nanofiltration membranes. *MRS Bulletin* **2008**, 33, 27-32.
- Campbell, P.; Srinivasan, R.; Knoell, T.; Phipps, D.; Ishida, R.; Safarik, J.; Cormack, T.; Ridgway, H.F. Quantitative structure activity relationship (QSAR) analysis of a *Mycobacterium* species to cellulose acetate and polyamide reverse osmosis membranes. *Biotechnol Bioengineering* **1999**, 64, 527-544.
- Childress, A.E.; Elimelech, M. Effect of solution chemistry on the surface charge of polymeric reverse osmosis and nanofiltration membranes. *J Membr Sci* **1996**, 119 (2), 253-268.
- Childress, A.E.; Elimelech, M. Relating nanofiltration membrane performance to membrane charge (electrokinetic) characteristics. *Environ Sci Technol* **2000**, 34 (17), 3710-3716.
- Cho, J.; Amy, G.; Pellegrino, J.; Yoon, Y. Characterization of clean and natural organic matter (NOM) fouled NF and UF membranes, and foulants characterization. *Desalination* **1998**, 118 (1-3) 101-108.

- Coronell, O.; Gonzalez, M.I.; Marinas, B.J.; Cahill, D.G. Ionization behavior, stoichiometry of association and accessibility of functional groups in the active layer of reverse osmosis and nanofiltration membranes. *Environ Sci Technol* **2010**, 44 (17), 6808-6814.
- Coronell, O.; Marinas, B.J.; Cahill, D.G. Depth heterogeneity of fully aromatic polyamide active layers in reverse osmosis and nanofiltration membranes. *Environ Sci Technol* **2011**, 45 (10), 4513-4520.
- Drelich, J.; Miller, J.D.; Good, R.J. The effect of drop (bubble) size on advancing and receding contact angles for heterogeneous and rough solid surfaces as observed with sessile-drop and captive-bubble techniques. *J Colloid Interf Sci* **1996**, 179 (1), 37-50.
- Freger, V. Nanoscale heterogeneity of polyamide membranes formed by interfacial polymerization. *Langmuir* **2003**, 19, 4791-4797.
- Gabelich, C.J.; Ishida, K.P.; Bold, R.M. Testing of water treatment copolymers for compatibility with polyamide reverse osmosis membranes. *Environ Prog* **2005**, 24 (4), 410-416.
- Gao, L.; McCarthy, T.J. Contact angle hysteresis explained. *Langmuir* **2006**, 22 (14), 6234-6237.
- Goosen, M.F.A.; Sablani, S.S.; Al-Hinai, H.; Al-Obeidani, S.; Al-Belushi, R.; Jackson, D. Fouling of reverse osmosis and ultrafiltration membranes: A critical review. *Sep Sci Technol* **2005**, 39 (10) 2261-2297.
- Greenlee, L.F.; Lawler, D.F.; Freeman, B.D.; Marrot, B.; Moulin, P. Reverse osmosis desalination: Water sources, technology and today's challenges. *Water Res* **2009**, 43, 2317-2348.
- Harrison, C.J.; Le Gouellec, Y.A.; Cheng, R.C.; Childress, A.E. Bench-scale testing of nanofiltration for seawater desalination. *J Environ Eng-ASCE* **2007**, 133 (11) 1004-1014.
- Herzberg, M.; Kang, S.; Elimelech, M. Role of extracellular polymeric substances (EPS) in biofouling of reverse osmosis membranes. *Environ Sci Technol* **2009** 43, 4393-4398.
- Hong, S.K.; Elimelech, M. Chemical and physical aspects of natural organic matter (NOM) fouling of nanofiltration membranes. *J Membr Sci* **1997**, 132 (2), 159-81.
- Hurwitz, G.; Guillen, G.R.; Hoek, E.M.V. Probing polyamide membrane surface charge, zeta potential, wettability and hydrophilicity with contact angle measurements. *J Membr Sci* **2010**, 349, 349-357.
- Jadav, G.L.; Aswal, V.K.; Singh, P.S. SANS study to probe nanoparticle dispersion in nanocomposite membranes of aromatic polyamide and functionalized silica nanoparticles. *J Colloid Interf Sci* **2010**, 351 (1) 304-314.
- Jeong, B-H.; Hoek, E.M.V.; Yan, Y.; Subramani, A.; Huang, X.; Hurwitz, G.; Ghosh, A.K.; Jawor, A. Interfacial polymerization of thin film nanocomposites: A new concept for reverse osmosis membranes. *J Membr Sci* **2007**, 294, 1-7.
- Kilduff, J.E.; Taniguchi, M.; Belfort, G. Low fouling synthetic membranes by UV-assisted graft polymerization: Monomer selection to mitigate fouling by natural organic matter. *J Membr Sci* **2003**, 222 (1-2) 59-70.

- Kim, J.; Van der Bruggen, B. The use of nanoparticles in polymeric and ceramic membrane structures: Review of manufacturing procedures and performance improvement for water treatment. *Environ Poll* **2010**, 158, 2335-2349.
- Kim, M.M.; Au, J.; Rahardianto, A.; Glater, J.; Cohen, Y.; Gerringer, F.W.; Gabelich, C.J. Impact of conventional water treatment coagulents on mineral scaling in RO desalting of brackish water. *Ind Eng Chem Res* **2009**, 48 (6), 3126-3135.
- Ladner, D.A.; Steele, M.; Weir, A.; Hristovski, K.; Westerhoff, P. Functionalized nanoparticles interactions with polymeric membranes. *J Hazard Mater* **2012**, in press.
- Lee, S.; Cho, J.; Elimelech, M. A novel method for investigating the influence of feed water recovery on colloidal and NOM fouling of RO and NF membranes. *Environ Eng Sci* **2005**, 22 (4), 496-509.
- Louie, J.S.; Pinnau, I.; Ciobanu, I.; Ishida, K.P.; Ng, A.; Reinhard, M. Effects of polyether-polyamide block copolymer coating on performance and fouling of reverse osmosis membranes. *J Membr Sci* **2006**, 280 (1-2), 762-770.
- Louie, J.S.; Pinnau, I.; Reinhard, M. Effects of surface coating process conditions on the water permeation and salt rejection properties of composite polyamide reverse osmosis membranes. *J Membr Sci* **2011**, 367 (1-2), 249-255.
- Luo, M.; Zhao, J.; Tang, W.; Pu, C. Hydrophilic modification of poly(ether sulfone) ultrafiltration membrane surface by self-assembly of TiO<sub>2</sub> nanoparticles. *Appl Surf Sci* **2005**, 249 (1-4), 76-84.
- Luxbacher, T. Electrokinetic characterization of flat sheet membranes by streaming current measurement. *Desalination* **2006**, 199, 376-377.
- Mi, B.; Elimelech, M. Organic fouling of forward osmosis membranes: Fouling reversibility and cleaning without chemical reagents. *J Membr Sci* **2009**, 348, 337-345.
- Michler, G.H. Scanning electron microscopy. In *Electron microscopy of polymers*; Pasch, H., Ed.; Springer: Berlin, 2008; pp 87-120.
- Minghao, G.; Kilduff, J.E.; Belfort, G. High throughput atmospheric pressure plasma-induced graft polymerization for identifying protein-resistant surfaces. *Biomaterials* **2012**, 33 (5), 1261-1270.
- Park, S-H.; Wei, S.; Mizaiko, B.; Taylor, A.E.; Favero, C.; Huang, C-H. Degradation of amine-based water treatment polymers during chloramination as *n*-nitrosodimethylamine (NDMA) precursors. *Environ Sci Technol* **2009**, 43 (5), 1360-1366.
- Petersen, R.J., Cadotte, J.E. Thin film composite reverse osmosis membrane. In *Handbook of Industrial Membrane Technology*; Porter, M.C., Ed.; Noyes Publication: New Jersey, 1990.
- Petry, M.; Sanz, M.A.; Langlais, C.; Bonnelye, V.; Durand, J.P.; Guevara, D.; Nardes, W.M.; Saemi, C.H. The El Coloso (Chile) reverse osmosis plant. *Desalination* **2007**, 203 (1-3) 141-152.
- Shannon, M.A.; Bohn, P.W.; Elimelech, M.; Georgiadis, J.G.; Marinas, B.J.; Mayes, A.M. Science and technology for water purification in the coming decades - A review. *Nature* **2008**, 452 (7185) 301-10.

- Siegbahn, K.M. Electron spectroscopy for atoms, molecules and condensed matter. In *Nobel Lectures, Physics 1981-1990*; Frängsmyr, T., Ed.; World Scientific Publishing Company: Singapore, 1993.
- Soroko, I.; Livingston, A. Impact of TiO<sub>2</sub> nanoparticles on morphology and performance of cross-linked polyimide organic solvent nanofiltration membranes. *J Membr Sci* **2009**, 343 (1-2) 189-198.
- Subramani, A.; Hoek, E.M. Direct observation of initial microbial deposition onto reverse osmosis and nanofiltration membranes. *J Membr Sci* **2008**, 319 (1-2), 111-125.
- Tang, C.Y.; Kwon, Y.N.; Leckie, J.O. Probing the nano- and micro-scales of reverse osmosis membranes – A comprehensive characterization of physicochemical properties of uncoated and coated membranes by XPS, TEM, ATR-FTIR, and streaming potential measurements. *J Membr Sci* **2007**, 287 (1), 146-156.
- Tang, C.Y.; Kwon, Y.N.; Leckie, J.O. Effect of membrane chemistry and coating layer on physicochemical properties of thin film composite polyamide RO and NF membranes I. FTIR and XPS characterization of polyamide and coating layer chemistry. *Desalination* **2009a**, 242 (1-3) 149-167.
- Tang, C.Y.; Kwon, Y.N.; Leckie, J.O. Effect of membrane chemistry and coating layer on physicochemical properties of thin film composite polyamide RO and NF membranes II. Membrane physicochemical properties and their dependence on polyamide and coating layers. *Desalination* **2009b**, 242 (1-3) 168-182.
- Taurozzi, J.S.; Arul, H.; Bosak, V.Z.; Burban, A.F.; Voice, T.C.; Bruening, M.L.; Tarabara, V.V. Effects of filler incorporation route on the properties of polysulfone-silver nanocomposite membranes of different porosities. *J Membr Sci* **2008**, 325 (1) 58-68.
- van der Bruggen, B.; Manttari, M.; Nystrom, M. Drawbacks of applying nanofiltration and how to avoid them: A review. *Sep Purif Technol* **2008**, 63 251-63.
- van de Lisdonk, C.A.C.; van Paassen, J.A.M.; Schippers, J.C. Monitoring scaling in nanofiltration and reverse osmosis membrane systems. *Desalination* **2000**, 132, 101-108.
- Xie, H.; Saito, T.; Hickner, M.A. Zeta potential of ion-conductive membranes by streaming current measurements. *Langmuir* **2011**, 27 (8) 4721-4727.
- Yan, L.; Li, Y.S.; Xiang, C.B.; Xianda, S. Effect of nano-sized Al<sub>2</sub>O<sub>3</sub>-particle addition on PVDF ultrafiltration membrane performance. *J Membr Sci* **2006**, 276 (1-2) 162-167.
- Yang, H.; Lin, J.C.; Huang, C. Application of nanosilver surface modification to RO membrane and space for mitigating biofouling in seawater desalination. *Water Res* **2009**, 43 (15) 3777-3786.
- Yang, Y.; Zhang, H.; Wang, P.; Zheng, Q.; Li, J. The influence of nano-sized TiO<sub>2</sub> fillers on the morphologies and properties of PSF UF membrane. *J Membr Sci* **2007**, 288 (1-2) 231-238.
- Zhou, M.; Liu, H.; Kilduff, J.E.; Langer, R.; Anderson, D.G.; Belfort, G. High-throughput membrane surface modification to control NOM fouling. *Environ Sci Technol* **2009**, 43 (10), 3865-3871.